Homeostatic feedback, not early activity, modulates development of two-state patterned activity in the *C. elegans* egg-laying circuit

Bhavya Ravi[1,2], Jessica Garcia[2], and Kevin M. Collins[1,2,3]

[1]Neuroscience Program, University of Miami Miller School of Medicine, Miami, FL USA

[2]Department of Biology, University of Miami, Coral Gables, FL USA

[3]To whom correspondence should be addressed:

kevin.collins@miami.edu

Department of Biology

University of Miami

1301 Memorial Drive

Coral Gables, FL 33143

Tel: (305) 284-9058

Website: www.bio.miami.edu/CollinsLab/

Twitter: @kevinemco

Short title: Development of *C. elegans* egg-laying circuit activity and behavior

63 pages with 9 Figures, 3 Supplemental Figures, 1 Supplemental Methods, 1 Supplementary Table, and 6 Supplementary Movies

Disclosures

The authors declare that no competing interests exist. BR, JG, and KMC performed experiments and data analysis, and BR and KMC wrote the paper.

Abstract

Neuron activity accompanies synapse formation and maintenance, but how early circuit activity contributes to behavior development is not well understood. Here, we use the *Caenorhabditis elegans* egg-laying motor circuit as a model to understand how coordinated cell and circuit activity develops and drives a robust two-state behavior in adults. Using calcium imaging in behaving animals, we find the Hermaphrodite Specific Neurons (HSNs) and vulval muscles show rhythmic Ca^{2+} transients in L4 larvae before eggs are produced. HSN activity in L4 is tonic and lacks the alternating burst-firing/quiescent pattern seen in egg-laying adults. Vulval muscle activity in L4 is initially uncoordinated, but becomes synchronous as the anterior and posterior muscle arms meet at HSN synaptic release sites. However, coordinated muscle activity does not require presynaptic HSN input. Using reversible silencing experiments, we show that neuronal and vulval muscle activity in L4 is not required for the onset of adult behavior. Instead, the accumulation of eggs in the adult uterus renders the muscles sensitive to HSN input. Sterilization or acute electrical silencing of the vulval muscles inhibits presynaptic HSN activity, and reversal of muscle silencing triggers a homeostatic increase in HSN activity and egg release that maintains ~12-15 eggs in the uterus. Feedback of egg accumulation depends upon the vulval muscle postsynaptic terminus, suggesting a retrograde signal sustains HSN synaptic activity and egg release. Thus, circuit development and activity is necessary but not sufficient to drive behavior without additional modulation by sensory feedback.

Key Words

Neural circuit, development, *C. elegans*, calcium, serotonin, neuromodulation, behavior

Significance

The functional importance of early, spontaneous neuron activity in synapse and circuit development is not well understood. Here we show that in the nematode *C. elegans*, the serotonergic Hermaphrodite Specific Neurons (HSNs) and postsynaptic vulval muscles show activity during circuit development, well before the onset of adult behavior. Surprisingly, early activity is not required for circuit development or the onset of adult behavior, and the circuit remains unable to drive egg laying until fertilized embryos are deposited into the uterus. Egg accumulation potentiates vulval muscle excitability, but ultimately acts to promote burst firing in the presynaptic HSNs. Our results suggest that mechanosensory feedback acts at three distinct steps to initiate, sustain, and terminate *C. elegans* egg-laying circuit activity and behavior.

Introduction

Developing neural circuits in the cortex, hippocampus, cerebellum, retina and spinal cord show spontaneous neural activity (1-5). In contrast, mature neural circuits show coordinated patterns of activity which are required to drive efficient behaviors. Activity-dependent mechanisms have been shown to play key roles during synapse formation and early neuronal development in vertebrates (6-10), but the complexity of such circuits poses limitations in terms of understanding how developmental events, neurotransmitter expression, and sensory signals act together to promote the transition from immature to mature patterns of circuit activity. Genetically tractable invertebrate model organisms, such as the nematode *Caenorhabditis elegans*, have simple neural circuits and are amenable to powerful experimental approaches allowing us to comprehensively investigate how activity in neural circuits is shaped during development and transitions to mature patterns of activity that drive behaviors.

The *C. elegans* egg laying circuit is a well-characterized neural circuit that drives a two-state behavior in adult animals with ~20 minute inactive periods punctuated by ~2 minute active states where ~5 eggs are laid (11). The egg-laying circuit consists of two serotonergic Hermaphrodite Specific Neurons (HSN) which promote the active state (11, 12), three locomotion motor neurons (VA7, VB6, and VD7) which may drive rhythmic input into the circuit (13), and six cholinergic Ventral C neurons (VC1-6), all of whom synapse onto a set of vulval muscles that contract to release eggs from the uterus (14). The *C. elegans* vulva develops post-embryonically into a toroidal organ that allows for the release of developing embryos into the external environment (15, 16). Four uv1 neuroendocrine cells connect the vulva canal to the uterus which holds embryos until they are laid.

HSN, VC, uv1, and vulval muscle development occurs during the early-mid L4 larval stages and requires interactions with the developing vulval epithelium, but not the other cells in the circuit (17-20). HSN-expressed SYG-1 interacts with SYG-2 expressed on the primary vulval epithelial cells, allowing proper HSN synapse placement (19, 20). The neurexin-related molecule BAM-2 is also expressed on the primary vulval epithelial cells and helps terminate VC4 and VC5 axon branching at the vulva (18). Extensions of the anterior and posterior vm2 vulval muscles, referred to as the lateral muscle arms, develop along the junction of the primary and secondary vulval epithelial cells, forming synapses with the HSN and VC boutons (21). LIN-12/Notch signaling in the vulval muscles directs the development of these vm2 muscle arms. Animals deficient in LIN-12/Notch signaling fail to develop vm2 muscle arms and are consequently egg-laying defective as adults because anterior and posterior vulval muscle contractility is asynchronous (21). Animals lacking HSNs or serotonin have prolonged egg-laying inactive states, indicating that serotonin modulates the onset of the egg laying active state (11). Serotonin released from the HSNs signals through vulval muscle receptors (22-26), likely increasing the electrical excitability of the muscles so that rhythmic input from cholinergic motors neurons can drive weak vulval muscle twitching or strong egg-laying contractions (13, 14, 27). Because each cell in the circuit develops independently in juveniles, how this circuit goes on to develop the robust pattern of coordinated activity seen in egg-laying adults remains unclear.

We have previously shown that HSN Ca^{2+} transients occur more frequently during the active state, but the factors which promote this timely ‘feed-forward’ increase in HSN activity remain poorly understood. The cholinergic VCs show little or no activity outside of

the active state. Within the active state, the VCs have rhythmic Ca^{2+} transients coincident with vulval muscle contractions, although whether VC activity drives contraction itself or instead acts to modulate HSN signaling is still not clear (28-31). The VCs also make synapses onto the body wall muscles, and optogenetic activation of the VCs leads to hypercontraction, suggesting that ACh released from VC might slow locomotion at the moment of egg release. Like the VCs, the uv1 neuroendocrine cells are active during egg laying. The uv1 cells, mechanically deformed by the passage of eggs through the vulva, release tyramine and neuropeptides that signal extrasynaptically to inhibit HSN activity (13, 32). Muscle activity in sterilized animals resembles that seen in the inactive state, suggesting that feedback of egg production or accumulation may influence whether and when animals enter the egg-laying active state.

Here, we leverage the experimental accessibility of the egg-laying circuit to investigate the relationship between cell activity, circuit development, and behavior development. We find the presynaptic HSN motor neurons and the postsynaptic vulval muscles are active during the late L4 larval stage, well before egg production and the onset of adult egg-laying behavior. We do not observe activity in the VC neurons and uv1 neuroendocrine cells until behavioral onset. The adult circuit remains in a non-functional state until receiving feedback that sufficient eggs have accumulated in the uterus. This egg-laying homeostat requires the vm2 muscle arms and muscle activity which promote HSN burst firing that maintains the active state. Together, our data show how cell activity patterns that emerge during development are modulated by sensory feedback that decide when and for how long to drive behavior.

Results

Asynchronous presynaptic and postsynaptic development in the *C. elegans* egg-laying behavior circuit. We have previously described the function of cell activity in the adult egg-laying behavior circuit and how developmental mutations impact circuit activity and adult behavior (13, 21, 27). Because development of the cells in the circuit is complete by the end of the fourth larval (L4) stage (33), we wanted to determine the relationship between cell activity and circuit development in juveniles and compare early activity to that seen in egg-laying adults. We exploited the stereotyped morphology of the developing primary and secondary vulval epithelial cells in the fourth (final) larval stage to define discrete half-hour stages of development as described (34). Fig. S1*A*-*D* shows vulval morphologies during the transition from L4.7 to L4.9 just prior to the L4-adult molt. The L4.7-8 larval transition lasted for ~1 hour, transitioning into the L4.8 ~0.5 h after Fig. S1*B* (right panel). The vulval lumen began to shrink in L4.8 and was fully collapsed by L4.9, ~0.5h later (Fig. S1*C*-*D*) (34). Vulval development was complete at the time of the final molt (Fig. S1*E*), and a fully formed vulva could be seen after cuticle shedding (Fig. S1*F*).

We find that HSN morphological and pre-synaptic development is complete prior to late L4 larval stages, confirming previous observations (17, 19, 20, 35). We expressed mCherry in HSNs from the NLP-3 neuropeptide promoter. We confirmed that the HSN axon had fasiculated and developed enlarged anterior and posterior synaptic boutons in L4.7-8 and L4.9 animals (arrowheads in Fig.1*A* and *B*). This organization is nearly identical to the HSN morphology seen in adults except that we sometimes detect a dorsal extension in adult animals that develops toward the position of the uv1 neuroendocrine

cells (third arrowhead in Fig.1*C*). GFP::RAB-3 expressed in HSN from the *unc-86* promoter showed clear punctate localization at synaptic sites in late L4 animals (Fig.1*D* and *E*), similar to that seen in adults (Fig.1*F*), suggesting that HSN presynaptic development is largely complete by L4.7-8.

Unlike HSNs, we found the post-synaptic vulval muscles completed their morphological development during the L4.9 stage, just prior to the L4 molt. We expressed mCherry in the vulval muscles from the *ceh-24* promoter (36) and found that the vm1 and vm2 vulval muscles were still developing at the L4.7-8 stage (Fig. 1*G*). After lumen collapse at the L4.9 stage, the tips of the vm1 muscles extended ventrally to the lips of the vulva, and the anterior and posterior vm2 muscle arms extended laterally along the junction between the primary and secondary vulval epithelial cells (Fig. 1*H*), making contact with each other at the HSN (and VC) synaptic release sites that continues in adults (Fig. 1*I*). Previous work has shown that mutations that disrupt LIN-12/Notch signaling perturb development of the vm2 muscle arms in late L4 animals, during the time when we observed vm2 muscle arm extension (21).

Vulval muscles express multiple receptors that might respond to serotonin released from HSN (22-26). In order to look at the developmental expression pattern of one such serotonin receptor, we examined a transgenic reporter line expressing GFP under the *ser-4b* gene promoter (37, 38). As shown in Fig 1*J* and 1*K*, we observed strong GFP expression in VulF and VulE primary and VulD secondary epithelial cells (20, 21). The *ser-4b* promoter also drove weak GFP expression in the vm2 muscles in L4.7-9, and this was elevated in adults (Fig. 1*J-L*). Previous serial EM reconstruction showed that HSN makes transient synapses onto the vulval epithelial cells in developing L4 animals

(20). Serotonin signaling through SER-4 may allow HSN (and possibly VC4 and VC5) to form temporary synapses onto the vulval epithelial cells until the vm2 muscle arms complete their lateral extension and form synapses. Consistent with this, *ser-4b* expression in adult animals was limited to the vm2 muscles (Fig. 1*L*). Lastly, we wanted to determine whether the VC motor neurons and uv1 neuroendocrine cells had completed their development in late L4 animals. To simultaneously visualize HSN, VC, and the uv1 neuroendocrine cells, we expressed mCherry from the *ida-1* promoter, a gene expressed in a subset of peptidergic cells, including those in the egg-laying circuit (39). As expected, HSN and VC presynaptic termini assembled at the junction between the primary and secondary vulval epithelial cells in L4.7-8. The uv1 cells were positioned laterally to the HSN/VC synaptic regions and extended dorsal processes around the primary vulval epithelial cells (Fig.1 *M-O*). These results indicate that the morphological development of the HSN, VC, and uv1 cells is largely complete by L4.7-8 stage. In contrast, vulval muscle development continues until after the L4.9 stage when the vm2 muscle arms reach each other and the HSN and the VC presynaptic boutons.

HSNs switch from tonic activity in juveniles to burst firing in egg-laying adults. We next wanted to determine if the HSNs show activity as they develop and how that activity compares to that seen in egg-laying adults. To follow HSN activity, we expressed the Ca^{2+} reporter GCaMP5 along with mCherry in HSN using the *nlp-3* promoter and performed ratiometric Ca^{2+} imaging as previously described (13). Starting at the L4.7-8 larval stage, we observed rhythmic Ca^{2+} activity in both HSN presynaptic termini and in the soma (Fig. 2*A* and 2*B*). During the L4.9 larval stage, when animals exhibited behavioral features of the developmentally timed L4 quiescence (40), rhythmic Ca^{2+} activity in HSNs slowed

(Fig. 2*B*; Movie S1). In adult animals, HSNs showed only infrequent activity during the egg-laying inactive state, but HSN activity switched to burst firing as animals entered the active state (Fig. 2*B*; Movie S2). We quantitated changes in HSN Ca^{2+} transient peak amplitude and frequency during the different developmental stages and behavior states. We found no significant differences in HSN Ca^{2+} transient amplitude (Fig. 2*C*), but we did observe significant changes in frequency. The median inter-transient interval in L4.7-8 animals was ~34s, and this interval increased to ~60s as animals reached the L4.9 stage (Fig. 2*D*). The reduction of HSN transient frequency seen in L4.9 animals resembled the egg-laying inactive state. However, none of the developmental stages recapitulated the 'burst' Ca^{2+} activity with <20 s inter-transient intervals seen during the egg-laying active state (Fig. 2*D*). Together, these results indicate that the HSNs show tonic Ca^{2+} activity once their morphological development is complete. HSN activity then switches into distinct inactive and active states as animals become egg-laying adults.

The onset of Ca^{2+} activity in the HSN neurons during the late L4 stage coincided with changes in animal locomotion, pharyngeal pumping, and defecation behaviors that accompany the L4 lethargus (40). Tonic HSN Ca^{2+} activity observed during late L4 was suppressed after the completion of the molt. In adults, serotonin release from the HSNs onto the AVF interneurons in the nerve ring has been shown to increase locomotor arousal during the egg-laying active state (41). We find the frequency of HSN transients decreases as L4.9 animals enter lethargus, consistent with a reduction in overall arousal and locomotion behavior. The ~50s rhythm of HSN activity in L4.9 animals resembles the defecation rhythm, prompting us to investigate whether there is a relationship between HSN activity and the defecation motor program (DMP). We found that defecation intervals

in L4.7-8 and adult animals were significantly longer when they were accompanied by one or more HSN Ca^{2+} transients (Fig. S2*A* and S2*B*). HSNs make and receive synapses from the excitatory GABAergic AVL motoneuron that regulates defecation, and serotonin and $G\alpha_o$ signaling have previously been shown to inhibit defecation behavior (14, 42). However, we found that optogenetic activation of the HSN neurons did not affect the defecation rhythm in L4 or adult animals (Fig. S2*C*). Two independent mutants lacking HSNs showed a significant decrease in DMP frequency (Fig. S2*D*), although this defecation phenotype was not observed in *egl-47(dm)* animals which also reduce HSN neurotransmitter release (43) . The egg-laying and defecation circuits both drive expulsion behaviors and are regulated by a common set of signaling molecules (44), but a role for HSN in coordinating these behaviors will require further study.

Vulval muscles Ca^{2+} transients increase in strength and frequency during development. Since HSN promotes vulval muscle activity and egg laying in adults, we wanted to determine if the HSN activity we observe in L4.7-8 and L4.9 animals drives early vulval muscle activity. We used the *ceh-24* promoter to drive expression of GCaMP5 and mCherry in the vulval muscles of L4 animals. We detected Ca^{2+} transients in the vulval muscles at the L4.7-8 larval stage (Fig. 3*A*; Movie S3), and these transients continued in L4.9 animals at increased frequency (Fig. 3*B-G*; Movies S4 and S5). The median interval between vulval muscle Ca^{2+} transients was ~32 s in L4.7-8 animals which dropped to 18 s in L4.9 animals. We compared juvenile activity to that seen in adults (Fig. *3D* and *3E*; Movie S6). Distributions of L4.9 Ca^{2+} transients were not significantly different from vulval muscle twitch transients seen in adults during the egg-laying inactive state (Fig. 3*G*). In contrast, the frequency of vulval muscle Ca^{2+} transients increased

significantly in animals during the egg-laying active state with median intervals dropping to ~7s phased with each body bend (Fig. 3*G*; (13)). We found that vulval muscle Ca^{2+} transients also become stronger during development. While Ca^{2+} transient amplitudes in the L4.7-8 and L4.9 stages were not significantly different, inactive phase Ca^{2+} transients of adults were stronger than those observed in L4 animals (Fig. 3*H*). In adult animals, strong Ca^{2+} transients were observed during the egg-laying active states, with the strongest Ca^{2+} transients driving the complete and simultaneous contraction of anterior and posterior vulval muscles to allow egg release (Fig. 3*E* and *H*).

We were surprised that vulval muscle transient frequencies decreased in adults as circuit activity bifurcated into distinct inactive and active egg-laying behavior states. Based on previous studies, we quantified periods of increased activity by measuring time spent with vulval muscle Ca^{2+} transient intervals less than one minute (27). We found that vulval muscle activity increased as L4.7-8 animals developed into L4.9 animals but then dropped significantly in egg-laying adults. L4.7-8 animals on average spent ~50% of their time in periods of increased vulval muscle activity, and this increased to 85% as animals entered the L4.9 stage (Fig. 3*I*). In contrast, adult animals spent only about ~33% of their time in periods with elevated vulval muscle activity (Fig. 3*I*) about half of which were coincident with the ~3 minute egg-laying active states that occur about every 20 minutes (11). What depresses vulval muscle activity in adult animals? We have previously shown that ERG K^+ channels inhibit vulval muscle excitability and egg-laying behavior (27). We found that expression of ERG from the vulval muscle-specific *unc-103e* promoter is low in L4 animals and increases as animals become adults (data not shown), providing a

266 molecular basis for the suppression of vulval muscle activity in adults that underlies
267 distinct inactive and active egg-laying behavior states.

268 **Development of coordinated vulval muscle activity for egg laying**. Egg release
269 through the vulva requires the synchronous contraction of the anterior (A) and posterior
270 (P) vulval muscles (Fig. 3*E*). Previous work has shown that loss of Notch signaling blocks
271 postsynaptic vm2 muscle arm development in L4 animals resulting in asynchronous
272 vulval muscle contractility and defects in egg-release in adults (21). Because of the vulval
273 slit, the lateral vm2 muscle arms that develop between L4.7-8 and L4.9 form the only sites
274 of potential contact between the anterior and posterior vulval muscles (Fig. 1*M* and 1*N*)
275 (13, 21). To determine the relationship between vulval muscle morphology and activity,
276 we examined the spatial distribution of vulval muscle Ca^{2+} during identified transients. We
277 found that only 5% of vulval muscle Ca^{2+} transients were coordinated in the L4.7-8 stage
278 (Fig. 3*A*; Movie S3), with nearly all transients occurring in either the anterior or posterior
279 muscles (Fig. 3*F* and 3*J*). The degree of vulval muscle coordination increased
280 significantly to ~28% of transients during L4.9 (Fig. *3J*; compare Movies S4 and S5) a
281 time when vm1 and vm2 muscles, as well as vm2 muscle arms, complete their
282 development (compare Fig. 1*M* and 1*N*). This level of coordinated muscle activity was not
283 significantly different to that found in adult animals during the egg-laying inactive state
284 (Fig. 3*J*; compare Fig. 3*C* and 3*D*). During the egg-laying active state ~60% of vulval
285 muscle transients were found to be coordinated, with Ca^{2+} transients occurring
286 synchronously in the anterior and posterior muscles (Movie S6). To test whether HSN
287 activity was required for the development of coordinated muscle activity, we analyzed
288 muscle activity in animals missing the HSNs. Surprisingly, we observed that vulval

289 muscles develop wild-type levels of coordinated activity even without HSN input (Fig. 3*J*).
290 We have previously shown that vulval muscle activity is phased with locomotion, possibly
291 via rhythmic ACh release from the VA7 and VB6 motor neurons onto the vm1 muscles
292 (13). Our results suggest that coordination of vulval muscle activity that develops by the
293 L4.9 stage, is independent of HSN input, and may instead be a consequence of A/P
294 muscle contact along the vulval slit and driven by input from the locomotion central pattern
295 generator.

296 **Early neuronal and vulval muscle activity is not required for the onset of adult egg-**
297 **laying behavior**. Activity in developing circuits has previously been shown to contribute
298 to mature patterns of activity that drive behavior. Is the activity we observe in HSN and
299 vulval muscles required for the proper onset of egg-laying behavior in adults? To test this,
300 we first set out to determine when adults initiate egg laying. Wild-type animals laid their
301 first egg at about ~6-7h after the L4-adult molt (Fig. 4*A*), a time when we first observed
302 VC and uv1 Ca^{2+} activity (data not shown). At this stage, animals had typically
303 accumulated ~8-10 eggs in the uterus. Animals without HSNs laid their first egg much
304 later, ~18 hours post molt (Fig. 4*A*). Gain-of-function receptor mutations which increase
305 inhibitory $G\alpha_o$ signaling in the HSNs (12, 29, 43) showed a delay in egg release until ~15-
306 17h after the L4 molt (Fig. 4*A*), resembling animals without HSNs. Surprisingly,
307 tryptophan hydroxylase *(tph-1*) knockout animals which are unable to synthesize
308 serotonin showed a small but significant delay in egg release compared to wild type (~7-
309 8h post L4 molt), suggesting that HSN promotes egg laying via release of
310 neurotransmitters other than serotonin.

To silence HSN and vulval muscle activity acutely and reversibly, we expressed *Drosophila* Histamine-gated chloride channels (HisCl) using cell-specific promoters and tested how histamine affected egg-laying behavior (45). Egg laying was unaffected by exogenous histamine in non-transgenic animals but was potently inhibited when HisCl channels were transgenically expressed in the HSNs, the vulval muscles, or in the entire nervous system (Fig. 4*B*). Silencing these cells in late L4 animals for the entire period where we observe activity caused no significant changes in the onset of adult egg laying after histamine washout in molted adults (Fig. 4*C*). We also observed no change in the steady-state number of unlaid eggs in the uterus after developmental silencing of L4 animals with histamine (data not shown). These results suggest that presynaptic and postsynaptic activity in the developing circuit is not required for circuit development or behavior.

Unlaid eggs promote vulval muscle responsiveness to HSN activity. We have previously shown that optogenetic activation of the HSNs in adult animals is sufficient to induce egg-laying circuit activity and behavior (13). Despite the fact that both the HSNs and vulval muscles show activity in L4.9 animals, egg laying does not begin until 6-7 hours later when the animals have accumulated ~8-10 unlaid eggs in the uterus. In order to dissect the relationship between egg production and circuit activity, we tested when the vulval muscles develop sensitivity to HSN input. We optogenetically activated the HSNs using Channelrhodopsin-2 (ChR2) while simultaneously recording Ca^{2+} activity in the vulval muscles at 3 stages: in L4.9 juveniles and in 3.5 h and 6.5 h adults. L4.9 animals have no eggs in the uterus, 3.5-hour adults contained 0-1 unlaid eggs, while 6.5-hour old adults had accumulated ~8-10 eggs. Stimulating HSNs in L4.9 juveniles or in 3.5-h adults

failed to induce detectable changes in vulval muscle Ca^{2+} activity (Fig. 5*A*, 5*B*, 5*D*). In contrast, optogenetic activation of HSNs in 6.5-hour adults significantly increased vulval muscle Ca^{2+} activity and triggered egg laying (Fig. 5*C* and 5*D*). The number of eggs in the uterus dictated the vulval muscle response to HSN activation. L4.9 or 3.5-hour adults with 0-1 eggs in the uterus had a mean transient frequency of ≤100 mHz, similar to the response seen in 6.5-hour adult animals with ~8 eggs grown without ATR. The vulval muscle Ca^{2+} response to HSN input was increased to ~170 mHz in 6-hour adults with ~8 unlaid eggs (Fig. 5*E*). The vulval muscles in serotonin-deficient mutants had a normal response to HSN activation at 6.5 hours (Fig. S3*A*-*C*), consistent with the normal onset of egg laying in these mutants (Fig. 4*A*). Together, these results show that the vulval muscles do not respond to HSN input until ~6.5 hours after the molt when fertilized embryos begin to accumulate in the uterus.

We next examined whether this change in vulval response in older adults was caused by ongoing developmental events or was instead a consequence of egg accumulation. We previously demonstrated that adults sterilized with FUDR, a chemical blocker of germline cell division and egg production, showed inactive state levels of vulval muscle activity (13). We found that vulval muscles in FUDR-treated animals were significantly less responsive to HSN optogenetic stimulation (Fig. 6*A* and 6*B*). The residual vulval muscle response in FUDR-treated animals is likely caused by incomplete sterilization when FUDR is added to L4.9 animals. We interpret these results as indicating that egg accumulation, not circuit maturity, modulates the onset of the egg-laying active state.

A retrograde signal of egg accumulation and vulval muscle activity drives presynaptic HSN activity. HSN activity can be inhibited by external sensory signals and feedback of egg release (12, 13, 29, 32), but the factors that promote HSN activity are not clear. We tested whether egg accumulation promotes circuit activity through the presynaptic HSNs, the postsynaptic vulval muscles, or both. We found that HSN Ca^{2+} activity, particularly the burst firing activity associated with the active state, was dramatically reduced in FUDR-treated animals (Fig. 7*A*). Although we did observe single HSN Ca^{2+} transients in FUDR treated animals, the intervals between were prolonged, often minutes apart (Fig. 7*C*). We quantified the total time spent by animals with HSN Ca^{2+} transient intervals <30s apart as a measure of HSN burst-firing seen in the active state. We found that while untreated animals spent ~13% of their time with the HSNs showing high-frequency activity, such bursts were eliminated in FUDR-treated animals (Fig. 7*D*). This result shows that feedback of egg production or accumulation modulates the frequency of HSN activity.

We performed a reciprocal experiment to test how electrical silencing of the postsynaptic vulval muscles affects presynaptic HSN activity. We have previously shown that passage of eggs through the vulva mechanically activates the uv1 neuroendocrine cells which release tyramine and neuropeptides that inhibit HSN activity and egg laying (13, 32). We hypothesized that prevention of egg release would block inhibitory uv1 feedback and increase HSN activity. We expressed HisCl channels in the vulval muscles and recorded HSN Ca^{2+} activity after silencing with exogenous histamine. Surprisingly, we found that acute silencing of vulval muscles significantly reduced presynaptic HSN Ca^{2+} activity, resembling FUDR treatment (Fig. 7*B* and 7*C*). While untreated animals

379 spent ~16% of recording time with high frequency HSN activity, this was reduced to ~2%
380 of the total recording time in histamine-treated animals (Fig. 7*D*). These results indicate
381 that vulval muscle activity is required for the burst firing in the HSN neurons that
382 accompanies the egg-laying active state.

383 We next looked at how HSN Ca^{2+} activity recovers when histamine inhibition of the
384 vulval muscles and egg laying is reversed. As shown in Fig. 8*A*, adult animals were
385 treated with or without histamine for 3-4 hours and then moved to plates without histamine
386 for a 20-30 minutes recovery period. Presynaptic HSN Ca^{2+} activity was then recorded as
387 the animals resumed egg-laying behavior. The HSNs showed a rapid and dramatic
388 recovery of Ca^{2+} activity after histamine washout resulting in a prolonged active state with
389 increased HSN Ca^{2+} transient frequency and numerous egg-laying events (Fig. 8*A* and
390 8*B*). Washout animals spent ~40% of their recorded time with elevated HSN activity
391 compared to 15% of untreated controls (Fig. 8*C*). During this recovery period, we
392 observed increased vulval muscle twitching contractions in the bright field channel,
393 indicating that muscle activity was restored (data not shown). These results suggest that
394 accumulation of unlaid eggs promotes vulval muscle activity which drives a homeostatic
395 increase in burst-firing pattern of HSN activity that sustains egg laying.

396 HSN synapses are formed exclusively on the vm2 muscle arms that provide sites
397 of contact between the anterior and posterior vulval muscles (14, 21, 27). Hypomorphic
398 Notch signaling mutants fail to develop vm2 muscle arms, and are egg-laying defective,
399 but have normal pre-synaptic HSN and VC development (21, 46). To determine if
400 retrograde signaling to the HSNs occurs through the vm2 muscle arms, we recorded HSN
401 Ca^{2+} activity in *lin-12(wy750)* Notch receptor mutant animals that are missing the vm2

muscle arms (Fig. 9*A* and 9*B*). We found that HSN Ca^{2+} transient frequency was strongly reduced in the *lin-12(wy750)* mutants compared to wild-type control animals (Fig. 9*C* and 9*D*). HSN Ca^{2+} transients still occurred in this mutant, but burst-firing was eliminated. Wild-type animals spent ~13% of their time with HSN transients <30s apart, while in the *lin-12(wy750)* mutant this was zero (Fig. 9*E*), resembling activity seen in FUDR-sterilized or vulval muscle-silenced animals. Together, these results indicate that muscle activity feeds back through the vm2 muscle arms onto the pre-synaptic HSN neurons to promote additional Ca^{2+} transients that drive burst firing and sustain the egg-laying active state.

Discussion

We used a combination of molecular genetic, optogenetic, and ratiometric Ca^{2+} imaging approaches to determine how coordinated activity develops in the *C. elegans* egg-laying behavior circuit. We find the pre-synaptic HSNs, VCs, and uv1 neuroendocrine cells complete morphological development in the early-mid L4 stages, while the vulval muscles finish developing at the late L4 stages. Like HSNs, the vulval muscles show Ca^{2+} activity in the L4.7-8 stage. Coordinated vulval muscle Ca^{2+} transients are not observed until the L4.9 stage, a time when the anterior and posterior vm2 muscle arms complete a Notch-dependent lateral extension around the primary vulval epithelial cells (21). We do not observe Ca^{2+} activity in the VC neurons and uv1 cells except in egg-laying adults (data not shown) suggesting activity in these cells does not contribute to circuit development. In adults, the juvenile HSN and vulval muscle activity disappears, leading to the establishment of characteristic ‘inactive’ states in which adult animals spend ~85% of their

time. Inactive state activity closely resembles that seen in sterilized animals that do not accumulate any eggs. We propose that uterine cells depress or excite the vulval muscles depending on the degree of stretch. Activation of the uterine muscles, which make gap junctions onto the vm2 muscles, would increase vulval muscle sensitivity to serotonin and other neurotransmitters released from HSN, which subsequently allows for rhythmic ACh input from the VA/VB locomotion motor neurons to drive vulval muscle Ca^{2+} activity. Coordinated Ca^{2+} activity in the anterior and posterior vulval muscles diffuses into the vm2 muscle arms to restimulate the HSNs and prolong the egg-laying active state. VC activity is coincident with strong vulval muscle contractions, while uv1 activity follows passage of eggs through the vulva. Once sufficient eggs have been laid, excitatory feedback to the vulval muscles and HSNs is reduced, increasing the probability that tyramine and neuropeptides released from VC and uv1 will block subsequent HSN Ca^{2+} transients, returning the circuit to the inactive state.

Changes in gene expression likely contribute to the changes in circuit activity patterns we observe between L4s and adults. Previous work has found that serotonin expression is low in L4 and increases as animals increase egg laying (47). Since mutants lacking serotonin have little effect on the timing of the first egg-laying event, we anticipate other neurotransmitters released from the HSNs promote egg laying in young adults. KCC-2 and ABTS-1, two Cl^- extruders required for inhibitory neurotransmission, show a developmental increase in HSN expression from L4 to adult (48, 49) which may be associated with the disappearance of spontaneous rhythmic activity in the HSNs after the late L4 stages. At the same time, we find that inhibitory ERG K^+ channel expression becomes strongly upregulated in the vulval muscles young adults. Mechanical stimuli are

447 also important regulators of transcription in developmental process such as tissue
448 patterning, cell fate determination, and differentiation (50). Studies in vertebrate models
449 have shown that stretch can increase the transcription of receptors that enhance muscle
450 contraction during parturition (51, 52). Cyclic stretch also regulates the expression of a
451 tissue specific gene, myocardin, in vascular smooth muscle cells (53). We speculate that
452 similar mechano-transcriptional mechanisms may operate in the *C. elegans* reproductive
453 system to drive expression of receptors and channels that modulate vulval muscle
454 sensitivity to presynaptic stimulation. Identifying additional genes whose expression
455 increases upon egg accumulation could help explain how HSN-deficient animals enter
456 the egg-laying active state.

457 The HSNs show dramatic changes in Ca^{2+} transient frequency between the
458 inactive and active states with little or no difference in transient amplitude. Previous work
459 has shown that the major G proteins, $G\alpha_q$ and $G\alpha_o$, signal in HSN to increase and inhibit
460 egg laying, respectively (29, 47). G protein signaling in HSN may modulate an intrinsic
461 pacemaker activity, similar to that seen in other central pattern generator circuits and in
462 the cardiac pacemaker (54). $G\alpha_o$ signaling in HSN activates inhibitory IRK K^+ channels
463 (12), and recent work has identified the T-type Ca^{2+} channel, CCA-1, and the Na^+ leak
464 channels, NCA-1 and NCA-2, as possible targets of excitatory $G\alpha_q$ signaling (31, 55, 56).
465 The balance of both G protein signaling pathways would allow for HSN frequency
466 modulation and dictate whether animals enter or leave the egg-laying active state.

467 Early vulval muscle activity may be spontaneous or driven by neuronal input.
468 Spontaneous Ca^{2+} transients promote the maturation of activity in many other cells (57).

We observed no change in behavioral onset or egg-laying rate in animals in which neuron or vulval muscle activity was silenced in the L4 stage. While this may result from incomplete silencing using the HisCl based approach, previous results indicate synapse development does not require Ca^{2+}-dependent excitatory transmission (58-60). While G protein signaling may drive early Ca^{2+} activity in the absence of electrical activity, synaptic transmission would still require Ca^{2+}-dependent vesicle fusion. The features of the vulval muscle Ca^{2+} transients we observe in juveniles are largely identical to that seen in adults. The persistence of activity in animals that lack HSNs or neural activity suggests they arise from a shared mechanism that is not required for synapse development and/or recovers quickly after histamine washout.

Our work continues to show the functional importance of the post-synaptic vm2 muscle arms in coordinating muscle activity during egg-laying behavior. Because of the intervening vulval slit through which eggs are laid, the vm2 muscle arms are the only sites of contact between the anterior and posterior muscles. Coordinated muscle Ca^{2+} transients appear during the L4.9 larval stage after vm2 muscle arm development. After development, the vm2 muscle arms may be electrically coupled at their points of contact, allowing for the immediate spread of electrical activity and/or Ca^{2+} signals between the anterior and posterior muscles. Mutants where the vm2 muscle arms fail to develop still have vm1 and vm2 Ca^{2+} activity, but this activity is uncoordinated (21). Additionally, these mutants do not show regenerative HSN Ca^{2+} activity, resembling the consequences of vulval muscle electrical silencing. The vm2 muscle arms also mediate synaptic input from HSN and VC. We have previously shown that the ERG K^+ channel and SER-1 serotonin receptor localize to the vm2 muscle arm region (21, 27). Both ERG and SER-1 have C-

terminal PDZ interaction motifs, and SER-1 has been shown to interact with the large PDZ scaffold protein MPZ-1 (61). Because gap junctions are potential targets of G protein signaling (62), innexin opening between neurons and muscles may facilitate the emergence of patterned 'burst' activity in the circuit that drives the egg-laying active state.

Neural circuits which generate directional movements during peristalsis, axial locomotion, and swimming rely on specialized central pattern generator (CPG) circuits which possess intrinsic rhythms (63). In these circuits, sensory feedback onto CPG micro-circuits as well as dedicated groups of interneurons regulate the spatio-temporal patterns of activation of motor neurons in adjacent body segments resulting in the sequential activation of muscles. Stretch signals and sensory feedback are essential for the coordination of activity in these cases. In *Drosophila*, the segmentally distributed GDL interneurons make synapses onto motor neurons which control wave propagation during larval locomotion. Feedback from stretch sensory neurons controls GDL activity and regulates the properties of wave propagation (64). In guinea-pigs, stretch-sensitive ascending and descending interneurons in the distal colon provide rhythmic excitatory and inhibitory inputs to enteric motor neurons during peristalsis (65). The *C. elegans* egg-laying system also appears to contain stretch-sensitive modalities, possibly relying on physiological mechanisms similar to those described above (66-68).

The VC motor neurons share key functional features of sensory neurons and interneurons which modulate CPG rhythms in other circuits. VC extends non-synaptic processes along the vulval hypodermis which could be mechanically activated by vulval muscle contraction (14, 18). The VC neurons make synapses onto both the vm2 vulval muscles and the body wall muscles. VC Ca^{2+} activity peaks at the moment of vulval

515 muscle contraction, but optogenetic activation of the VCs fails to elicit egg laying events
516 and instead slows locomotion. Moreover, VC- and acetylcholine-defective mutants show
517 increased egg laying (28, 29), suggesting a loss of inhibitory feedback. Thus, the VCs,
518 instead of releasing acetylcholine at the vm2 synapse to drive vulval muscle contraction,
519 may function in part as baroreceptors to slow locomotion during egg release (13). This
520 mode of action is similar to the mechanosensory gastric-pyloric receptor (GPR) cells in
521 crabs which are rhythmically activated by muscle movements in the foregut, and release
522 ACh and serotonin onto CPG neurons in the stomatogastric ganglion (STG). This
523 simultaneously elicits fast excitatory and slow modulatory changes in the firing properties
524 of STG neurons (69). Our studies of the egg-laying circuit show that ongoing HSN activity
525 depends on a signal released from the post-synaptic vulval muscles induced by stretch-
526 dependent activation. Further studies of the egg-laying circuit should allow for the
527 identification of the molecules and cells that drive this unique form of retrograde
528 modulation of presynaptic activity.

529

Materials and Methods

Nematode Culture and Developmental Staging. *Caenorhabditis elegans* hermaphrodites were maintained at 20°C on Nematode Growth Medium (NGM) agar plates with *E. coli* OP50 as a source of food as described (70). Animals were staged and categorized based on the morphology of the vulva as described in the results section. For assays involving young adults, animals were age-matched based on the timing of completion of the L4 larval molt. All assays involving adult animals were performed using age-matched adult hermaphrodites 20-40 hours past the late L4 stage.

Confocal Microscopy and Ratiometric Ca^{2+} Imaging. To visualize the egg-laying system, L4s and age-matched adults were immobilized using 10 mM muscimol on 4% agarose pads and covered with #1 coverslips. Two-channel confocal Z-stacks (along with a bright-field channel) using a pinhole opening of 1 Airy Unit (0.921µm thick optical sections, 16-bit images) were obtained with an inverted Leica TCS SP5 confocal microscope with a 63X Water Apochromat objective (1.2NA). Ca^{2+} recordings were made using the 8kHz resonant scanner and the pinhole opened for ~20µm optical slices. Recordings were collected at ~20 fps at 256x256 pixel resolution, 12-bit depth and ≥2X digital zoom using a 20x Apochromat objective (0.7NA). GFP/GCaMP5 and mCherry fluorescence was excited using a 488 nm and 561 nm laser lines, respectively. L4 animals at the relevant stages of vulval development were identified based on vulval morphology (34). Adult recordings were performed 24 hours after the late L4 stage. Young adults (3.5–6.5 h) were staged after cuticle shedding at the L4 to adult molt. After staging, animals were allowed to adapt for ~30 min before imaging. During imaging, the stage and focus were adjusted manually to keep the relevant cell/pre-synapse in view and in focus.

553 Ratiometric analysis for all Ca^{2+} recordings was performed using Volocity 6.3.1
554 (Perkin Elmer) as described (13). The egg-laying active state was operationally defined
555 as the period one minute prior to the first egg-laying event, and ending one minute after
556 the last (in the case of a typical active phase where 3-4 eggs are laid in quick succession).
557 However, in cases where two egg-laying events were apart by >60 seconds, peaks were
558 considered to be in separate active phases and transients between these were
559 considered to be from the inactive state. To facilitate comparisons of ΔR/R between
560 different reporters, developmental stages, and recording conditions, HSN recordings in
561 which baseline GCaMP5/mCherry fluorescence ratio values were between 0.2-0.3 were
562 selected for the analysis, while vulval muscle recordings with GCaMP5/mCherry ratio
563 values between 0.1-0.2 were chosen (≥80% of recordings). The coordination of vulval
564 muscle contraction was determined as described (21).

565 **Behavior Assays and Microscopy**. ChR2 expressing strains were maintained on OP50
566 with or without all-*trans* retinal (ATR) (0.4 mM). ChR2 was activated during Ca^{2+} imaging
567 experiments with the same laser light used to excite GCaMP5 fluorescence. For acute
568 silencing assays, NGM plates containing 10 mM histamine were prepared and used as
569 described (45). For adult behavioral assays, HisCl expressing strains were staged as late
570 L4s with assays performed 24 hours later. For L4 activity silencing, L4.7 animals were
571 placed on NGM plates with or without 10 mM histamine and were monitored to note when
572 the animals complete the L4 molt. Each animal was then transferred to a new seeded
573 plate, and the time for each animal to lay its first egg was recorded. Animals were
574 sterilized using Floxuridine (FUDR); 100 µl of 10mg/ml FUDR was applied to OP50

seeded NGM plates. Late L4 animals were then staged onto the FUDR plates and sterilized adults were imaged 24 hours later.

Statistical Analysis. Statistical analysis was performed using Prism 6 (GraphPad). Sample sizes for behavioral assays followed previous studies (13, 27, 71). Ca^{2+} transient peak amplitudes, widths, and inter-transient intervals were pooled from multiple animals (typically ~10 animals per genotype/condition per experiment). Individual *p* values are indicated in each Figure legend, and all tests were corrected for multiple comparisons (Bonferroni for ANOVA; Dunn for Kruskal-Wallis).

ACKNOWLEDGEMENTS. This work was funded by a grant from NINDS to KMC (R01 NS086932). JG was supported by the Bridge to the Baccalaureate Program (R25 GM050083). Strains used in this study have been provided to the *C. elegans* Genetics Center, which is funded by NIH Office of Research Infrastructure Programs (P40 OD010440). We thank Addy Bode and Michael Scheetz for help with strain construction. We thank James Baker, Julia Dallman, and members of the Collins lab and for helpful discussions and feedback.

References:

1. Garaschuk O, Hanse E, & Konnerth A (1998) Developmental profile and synaptic origin of early network oscillations in the CA1 region of rat neonatal hippocampus. *J Physiol* 507 (Pt 1):219-236.
2. Garaschuk O, Linn J, Eilers J, & Konnerth A (2000) Large-scale oscillatory calcium waves in the immature cortex. *Nat Neurosci* 3(5):452-459.
3. Warp E*, et al.* (2012) Emergence of patterned activity in the developing zebrafish spinal cord. *Curr Biol* 22(2):93-102.
4. Watt AJ*, et al.* (2009) Traveling waves in developing cerebellar cortex mediated by asymmetrical Purkinje cell connectivity. *Nat Neurosci* 12(4):463-473.
5. Wong RO, Chernjavsky A, Smith SJ, & Shatz CJ (1995) Early functional neural networks in the developing retina. *Nature* 374(6524):716-718.
6. Borodinsky LN*, et al.* (2004) Activity-dependent homeostatic specification of transmitter expression in embryonic neurons. *Nature* 429(6991):523-530.
7. Gu X, Olson EC, & Spitzer NC (1994) Spontaneous neuronal calcium spikes and waves during early differentiation. *J Neurosci* 14(11 Pt 1):6325-6335.
8. Gu X & Spitzer NC (1995) Distinct aspects of neuronal differentiation encoded by frequency of spontaneous Ca^{2+} transients. *Nature* 375(6534):784-787.
9. Hanson MG, Milner LD, & Landmesser LT (2008) Spontaneous rhythmic activity in early chick spinal cord influences distinct motor axon pathfinding decisions. *Brain Res Rev* 57(1):77-85.
10. Jarecki J & Keshishian H (1995) Role of neural activity during synaptogenesis in *Drosophila*. *J Neurosci* 15(12):8177-8190.

614 11. Waggoner LE, Zhou GT, Schafer RW, & Schafer WR (1998) Control of alternative
615 behavioral states by serotonin in *Caenorhabditis elegans*. *Neuron* 21(1):203-214.
616 12. Emtage L*, et al.* (2012) IRK-1 potassium channels mediate peptidergic inhibition
617 of *Caenorhabditis elegans* serotonin neurons via a G(o) signaling pathway. *J*
618 *Neurosci* 32(46):16285-16295.
619 13. Collins KM*, et al.* (2016) Activity of the *C. elegans* egg-laying behavior circuit is
620 controlled by competing activation and feedback inhibition. *Elife* 5:e21126.
621 14. White JG, Southgate E, Thomson JN, & Brenner S (1986) The structure of the
622 nervous system of the nematode *Caenorhabditis elegans*. *Philos Trans R Soc*
623 *Lond B Biol Sci* 314(1165):1-340.
624 15. Schindler AJ & Sherwood DR (2013) Morphogenesis of the *Caenorhabditis*
625 *elegans* vulva. *Wiley Interdiscip Rev Dev Biol* 2(1):75-95.
626 16. Sternberg PW (2005) Vulval development. *WormBook*:1-28.
627 17. Adler CE, Fetter RD, & Bargmann CI (2006) UNC-6/Netrin induces neuronal
628 asymmetry and defines the site of axon formation. *Nat Neurosci* 9(4):511-518.
629 18. Colavita A & Tessier-Lavigne M (2003) A Neurexin-related protein, BAM-2,
630 terminates axonal branches in *C. elegans*. *Science* 302(5643):293-296.
631 19. Shen K & Bargmann CI (2003) The immunoglobulin superfamily protein SYG-1
632 determines the location of specific synapses in *C. elegans*. *Cell* 112(5):619-630.
633 20. Shen K, Fetter RD, & Bargmann CI (2004) Synaptic specificity is generated by the
634 synaptic guidepost protein SYG-2 and its receptor, SYG-1. *Cell* 116(6):869-881.

635 21. Li P, Collins KM, Koelle MR, & Shen K (2013) LIN-12/Notch signaling instructs
636 postsynaptic muscle arm development by regulating UNC-40/DCC and MADD-2
637 in *Caenorhabditis elegans*. *Elife* 2:e00378.
638 22. Carnell L, Illi J, Hong SW, & McIntire SL (2005) The G-protein-coupled serotonin
639 receptor SER-1 regulates egg laying and male mating behaviors in *Caenorhabditis*
640 *elegans*. *J Neurosci* 25(46):10671-10681.
641 23. Dempsey CM, Mackenzie SM, Gargus A, Blanco G, & Sze JY (2005) Serotonin
642 (5HT), fluoxetine, imipramine and dopamine target distinct 5HT receptor signaling
643 to modulate *Caenorhabditis elegans* egg-laying behavior. *Genetics* 169(3):1425-
644 1436.
645 24. Dernovici S, Starc T, Dent JA, & Ribeiro P (2007) The serotonin receptor SER-1
646 (5HT2ce) contributes to the regulation of locomotion in *Caenorhabditis elegans*.
647 *Dev Neurobiol* 67(2):189-204.
648 25. Hapiak VM*, et al.* (2009) Dual excitatory and inhibitory serotonergic inputs
649 modulate egg laying in *Caenorhabditis elegans*. *Genetics* 181(1):153-163.
650 26. Hobson RJ*, et al.* (2006) SER-7, a *Caenorhabditis elegans* 5-HT7-like receptor, is
651 essential for the 5-HT stimulation of pharyngeal pumping and egg laying. *Genetics*
652 172(1):159-169.
653 27. Collins KM & Koelle MR (2013) Postsynaptic ERG potassium channels limit
654 muscle excitability to allow distinct egg-laying behavior states in *Caenorhabditis*
655 *elegans*. *J Neurosci* 33(2):761-775.

656 28. Bany IA, Dong MQ, & Koelle MR (2003) Genetic and cellular basis for acetylcholine
657 inhibition of *Caenorhabditis elegans* egg-laying behavior. *J Neurosci* 23(22):8060-
658 8069.
659 29. Ringstad N & Horvitz HR (2008) FMRFamide neuropeptides and acetylcholine
660 synergistically inhibit egg-laying by *C. elegans*. *Nat Neurosci* 11(10):1168-1176.
661 30. Schafer WR, Sanchez BM, & Kenyon CJ (1996) Genes affecting sensitivity to
662 serotonin in *Caenorhabditis elegans*. *Genetics* 143(3):1219-1230.
663 31. Zang KE, Ho E, & Ringstad N (2017) Inhibitory peptidergic modulation of *C.*
664 *elegans* serotonin neurons is gated by T-type calcium channels. *Elife* 6:e22771.
665 32. Banerjee N, Bhattacharya R, Gorczyca M, Collins KM, & Francis MM (2017) Local
666 neuropeptide signaling modulates serotonergic transmission to shape the
667 temporal organization of *C. elegans* egg-laying behavior. *PLoS Genet*
668 13(4):e1006697.
669 33. Li C & Chalfie M (1990) Organogenesis in *C. elegans*: positioning of neurons and
670 muscles in the egg-laying system. *Neuron* 4(5):681-695.
671 34. Mok DZ, Sternberg PW, & Inoue T (2015) Morphologically defined sub-stages of
672 *C. elegans* vulval development in the fourth larval stage. *BMC Dev Biol* 15:26.
673 35. Patel MR, *et al.* (2006) Hierarchical assembly of presynaptic components in
674 defined *C. elegans* synapses. *Nat Neurosci* 9(12):1488-1498.
675 36. Harfe BD & Fire A (1998) Muscle and nerve-specific regulation of a novel NK-2
676 class homeodomain factor in *Caenorhabditis elegans*. *Development* 125(3):421-
677 429.

678 37. Gurel G, Gustafson MA, Pepper JS, Horvitz HR, & Koelle MR (2012) Receptors
679 and other signaling proteins required for serotonin control of locomotion in
680 *Caenorhabditis elegans*. *Genetics* 192(4):1359-1371.
681 38. Tsalik EL & Hobert O (2003) Functional mapping of neurons that control
682 locomotory behavior in *Caenorhabditis elegans*. *J Neurobiol* 56(2):178-197.
683 39. Cai T, Fukushige T, Notkins AL, & Krause M (2004) Insulinoma-Associated Protein
684 IA-2, a Vesicle Transmembrane Protein, Genetically Interacts with UNC-31/CAPS
685 and Affects Neurosecretion in *Caenorhabditis elegans*. *J Neurosci* 24(12):3115-
686 3124.
687 40. Raizen DM*, et al.* (2008) Lethargus is a *Caenorhabditis elegans* sleep-like state.
688 *Nature* 451(7178):569-572.
689 41. Hardaker LA, Singer E, Kerr R, Zhou G, & Schafer WR (2001) Serotonin modulates
690 locomotory behavior and coordinates egg-laying and movement in *Caenorhabditis*
691 *elegans*. *J Neurobiol* 49(4):303-313.
692 42. Segalat L, Elkes DA, & Kaplan JM (1995) Modulation of serotonin-controlled
693 behaviors by Go in *Caenorhabditis elegans*. *Science* 267(5204):1648-1651.
694 43. Moresco JJ & Koelle MR (2004) Activation of EGL-47, a Galpha(o)-coupled
695 receptor, inhibits function of hermaphrodite-specific motor neurons to regulate
696 *Caenorhabditis elegans* egg-laying behavior. *J Neurosci* 24(39):8522-8530.
697 44. Reiner DJ & Thomas JH (1995) Reversal of a muscle response to GABA during
698 *C. elegans* male development. *J Neurosci* 15(9):6094-6102.

699 45. Pokala N, Liu Q, Gordus A, & Bargmann CI (2014) Inducible and titratable silencing
700 of *Caenorhabditis elegans* neurons in vivo with histamine-gated chloride channels.
701 *Proc Natl Acad Sci U S A* 111(7):2770-2775.
702 46. Sundaram M & Greenwald I (1993) Suppressors of a lin-12 hypomorph define
703 genes that interact with both lin-12 and glp-1 in *Caenorhabditis elegans*. *Genetics*
704 135(3):765-783.
705 47. Tanis JE, Moresco JJ, Lindquist RA, & Koelle MR (2008) Regulation of serotonin
706 biosynthesis by the G proteins Galphao and Galphaq controls serotonin signaling
707 in *Caenorhabditis elegans*. *Genetics* 178(1):157-169.
708 48. Bellemer A, Hirata T, Romero MF, & Koelle MR (2011) Two types of chloride
709 transporters are required for GABA(A) receptor-mediated inhibition in *C. elegans*.
710 *EMBO J* 30(9):1852-1863.
711 49. Tanis JE, Bellemer A, Moresco JJ, Forbush B, & Koelle MR (2009) The potassium
712 chloride cotransporter KCC-2 coordinates development of inhibitory
713 neurotransmission and synapse structure in *Caenorhabditis elegans*. *J Neurosci*
714 29(32):9943-9954.
715 50. Mammoto A, Mammoto T, & Ingber DE (2012) Mechanosensitive mechanisms in
716 transcriptional regulation. *J Cell Sci* 125(Pt 13):3061-3073.
717 51. Shynlova O*, et al.* (2007) Uterine stretch regulates temporal and spatial expression
718 of fibronectin protein and its alpha 5 integrin receptor in myometrium of unilaterally
719 pregnant rats. *Biol Reprod* 77(5):880-888.

720 52. Terzidou V*, et al.* (2005) Mechanical stretch up-regulates the human oxytocin
721 receptor in primary human uterine myocytes. *J Clin Endocrinol Metab* 90(1):237-
722 246.
723 53. Chiu CZ, Wang BW, & Shyu KG (2013) Effects of cyclic stretch on the molecular
724 regulation of myocardin in rat aortic vascular smooth muscle cells. *J Biomed Sci*
725 20:50.
726 54. Hille B (2001) *Ion Channels of Excitable Membranes* (Sinaur) Third Ed.
727 55. Topalidou I*, et al.* (2012) Genetically separable functions of the MEC-17 tubulin
728 acetyltransferase affect microtubule organization. *Curr Biol* 22(12):1057-1065.
729 56. Yeh E*, et al.* (2008) A putative cation channel, NCA-1, and a novel protein, UNC-
730 80, transmit neuronal activity in *C. elegans*. *PLoS Biol* 6(3):e55.
731 57. Moody WJ & Bosma MM (2005) Ion channel development, spontaneous activity,
732 and activity-dependent development in nerve and muscle cells. *Physiol Rev*
733 85(3):883-941.
734 58. Lu W, Bushong EA, Shih TP, Ellisman MH, & Nicoll RA (2013) The cell-
735 autonomous role of excitatory synaptic transmission in the regulation of neuronal
736 structure and function. *Neuron* 78(3):433-439.
737 59. Sando R*, et al.* (2017) Assembly of Excitatory Synapses in the Absence of
738 Glutamatergic Neurotransmission. *Neuron* 94(2):312-321 e313.
739 60. Verhage M*, et al.* (2000) Synaptic assembly of the brain in the absence of
740 neurotransmitter secretion. *Science* 287(5454):864-869.

741 61. Xiao H*, et al.* (2006) SER-1, a *Caenorhabditis elegans* 5-HT2-like receptor, and a
742 multi-PDZ domain containing protein (MPZ-1) interact in vulval muscle to facilitate
743 serotonin-stimulated egg-laying. *Dev Biol* 298(2):379-391.
744 62. Correa PA, Gruninger T, & Garcia LR (2015) DOP-2 D2-Like Receptor Regulates
745 UNC-7 Innexins to Attenuate Recurrent Sensory Motor Neurons during *C. elegans*
746 Copulation. *J Neurosci* 35(27):9990-10004.
747 63. Grillner S (2003) The motor infrastructure: from ion channels to neuronal networks.
748 *Nat Rev Neurosci* 4(7):573-586.
749 64. Fushiki A*, et al.* (2016) A circuit mechanism for the propagation of waves of muscle
750 contraction in *Drosophila*. *Elife* 5:13253.
751 65. Spencer NJ, Dickson EJ, Hennig GW, & Smith TK (2006) Sensory elements within
752 the circular muscle are essential for mechanotransduction of ongoing peristaltic
753 reflex activity in guinea-pig distal colon. *J Physiol* 576(Pt 2):519-531.
754 66. Hu Z, Pym EC, Babu K, Vashlishan Murray AB, & Kaplan JM (2011) A
755 neuropeptide-mediated stretch response links muscle contraction to changes in
756 neurotransmitter release. *Neuron* 71(1):92-102.
757 67. Li W, Feng Z, Sternberg PW, & Xu XZ (2006) A *C. elegans* stretch receptor neuron
758 revealed by a mechanosensitive TRP channel homologue. *Nature* 440(7084):684-
759 687.
760 68. Wen Q*, et al.* (2012) Proprioceptive coupling within motor neurons drives *C.*
761 *elegans* forward locomotion. *Neuron* 76(4):750-761.

762 69. Katz PS & Harris-Warrick RM (1990) Neuromodulation of the crab pyloric central
763 pattern generator by serotonergic/cholinergic proprioceptive afferents. *J Neurosci*
764 10(5):1495-1512.
765 70. Brenner S (1974) The genetics of *Caenorhabditis elegans*. *Genetics* 77(1):71-94.
766 71. Chase DL, Pepper JS, & Koelle MR (2004) Mechanism of extrasynaptic dopamine
767 signaling in *Caenorhabditis elegans*. *Nat Neurosci* 7(10):1096-1103.

768

769

770

771

772

773

774

775

776

777

778

779

Figure Legends

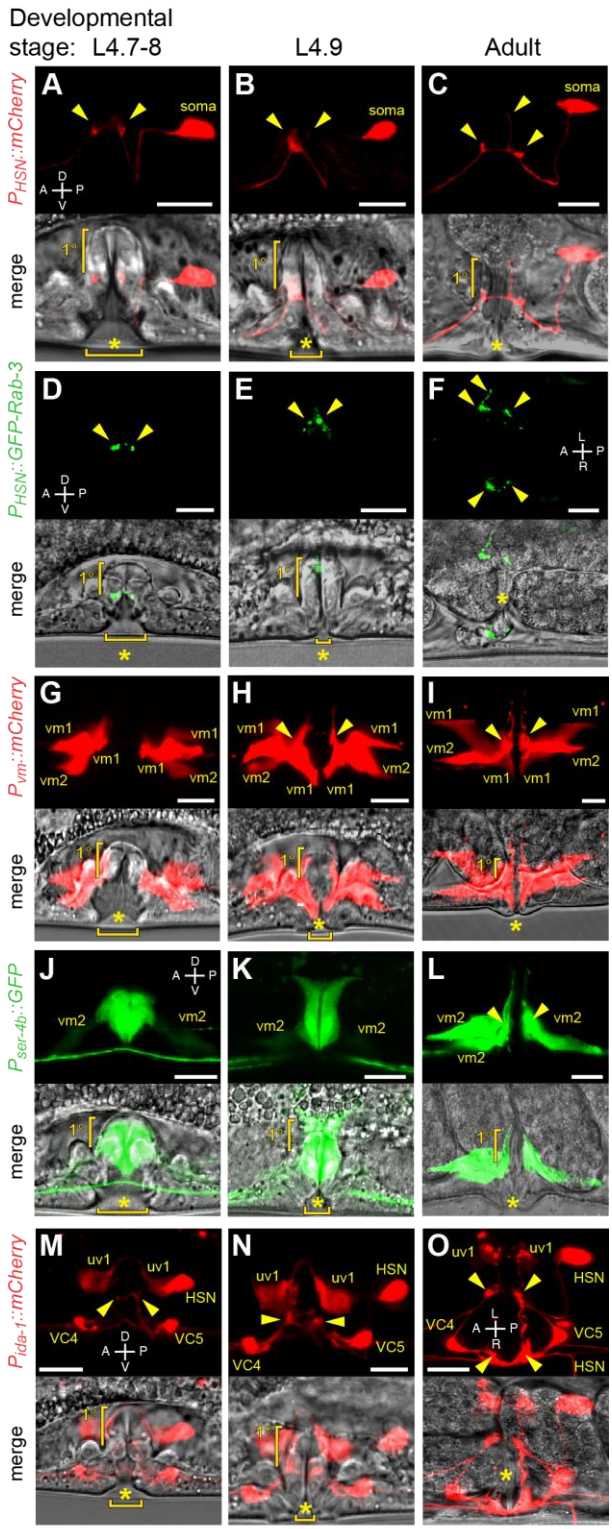

Fig. 1: Morphological development of the *C. elegans* egg-laying circuit. (*A-C*) Morphology of HSN (top) and vulva (bottom) in L4.7-8 (*A*) and L4.9 (*B*) larval stages

and in adults (*C*). (*D-F*) Morphology of HSN synapses (top) and vulva (bottom) in L4.7-8 (*C*) and L4.9 (*D*) larval stages and in adults (*E*). Arrowheads indicate RAB-3-GFP presynaptic puncta. (*G-I*) Morphology of vm1 and vm2 vulval muscles (top) and vulva (bottom) in L4.7-8 (*G*) and L4.9 (*H*) larval stages and in adults (*I*). (*J-L*) Developmental expression of *ser-4* from a GFP transcriptional reporter at the L4.7-8 (*J*) and L4.9 (*K*) larval stages and in adults (*L*). (*M-O*) Morphology of HSN, VC4, VC5, and the uv1 neuroendocrine cells (top) and vulva (bottom) in L4.7-8 (*M*) and L4.9 (*N*) larval stages and in adults (*O*) visualized using the *ida-1* promoter. Arrowheads in all images indicate the location of presynaptic boutons or postsynaptic vm2 muscle arms. Scale bar is 10 µm, and asterisk indicates the position of the developing or completed vulval opening. Vertical half-brackets indicate the approximate position of primary (1°) vulval epithelial cells, and horizontal bracket indicates progress of vulval lumen collapse at each larval stage.

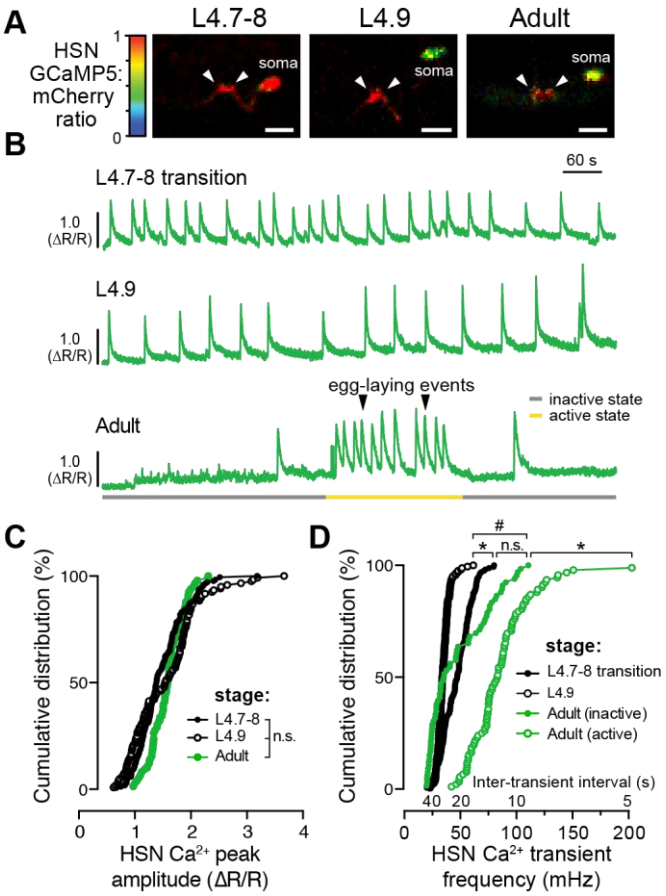

811

812 **Fig. 2. HSN neurons show tonic Ca^{2+} activity during the late L4 stage and burst**
813 **firing during the egg-laying active state.** (*A*) Micrographs of the intensity-modulated
814 GCaMP5:mCherry fluorescence ratio during HSN Ca^{2+} transients in L4.7-8 and L4.9
815 larval stages, and in adults. White arrowheads show Ca^{2+} activity localized to the anterior
816 and posterior presynaptic boutons. Scale bar is 10µm; anterior is at left, ventral is at
817 bottom. See also Movies S1 and S2. (*B*) Representative GCaMP5:mCherry ratio traces
818 (ΔR/R) of HSN Ca^{2+} activity in L4.7-8 (top), L4.9 (middle), and in adult animals (bottom).
819 Adults show distinct active (yellow) and inactive (grey) egg-laying behavior states. Black
820 arrowheads indicate egg-laying events. (*C*) Cumulative distributions of HSN Ca^{2+} peak
821 amplitudes in L4.7-8 (closed black circles), L4.9 (open black circles), and adults (closed

822 green circles). n.s. indicates p>0.0809 (one-way ANOVA). (*D*) Cumulative distribution
823 plots of instantaneous HSN Ca^{2+} transient frequencies (and inter-transient intervals) from
824 L4.7-8 (closed black circles) and L4.9 (open black circles) animals, and from adult egg-
825 laying inactive (green closed circles) and active (green open circles) states. Asterisks (*)
826 indicate p<0.0001; pound sign (#) indicates p=0.0283; n.s. indicates p=0.1831 (Kruskal-
827 Wallis test).

828

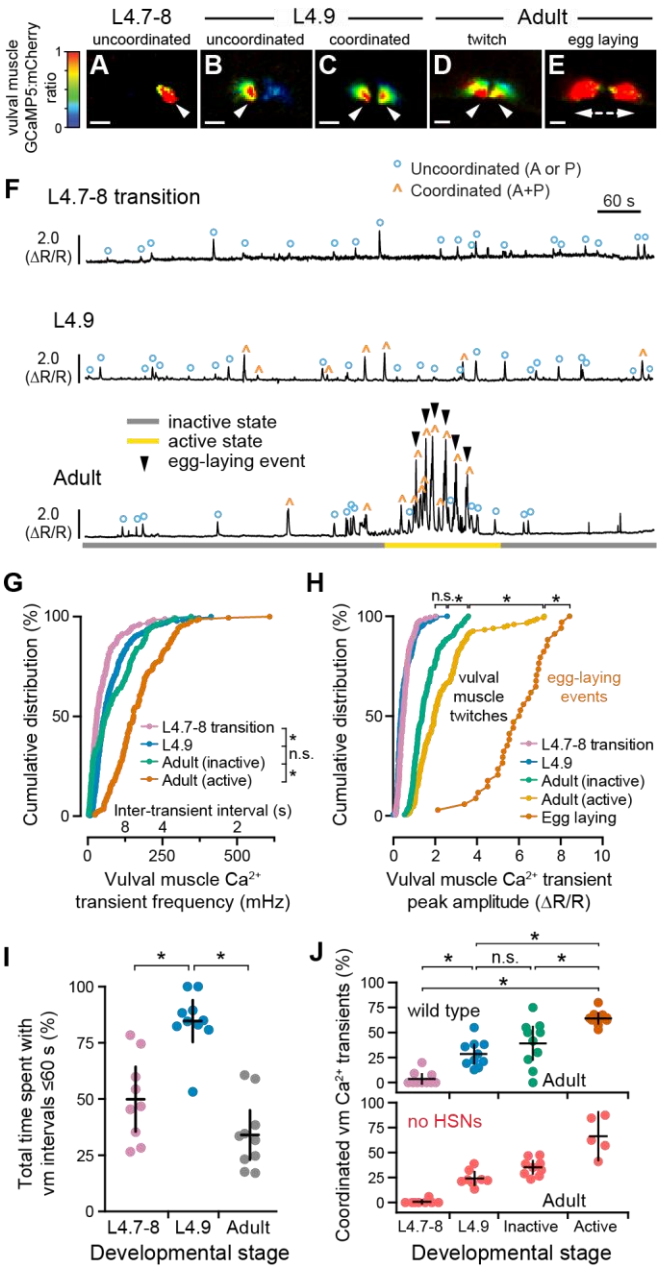

829

830 **Fig. 3. Development of coordinated vulval muscle Ca^{2+} transients in the L4.9 stage**
831 **does not require presynaptic HSN input.** (*A-E*) Micrographs of GCaMP5:mCherry
832 fluorescence ratio during vulval muscle Ca^{2+} transients at the L4.7-8 (*A*), L4.9 larval
833 stages (*B*,*C*), and during the adult active state (*D*,*E*). White arrowheads show localization
834 of Ca^{2+} transients. Scale bars are 10 µm; anterior at left, ventral at bottom. See also

835 Movies S3-6. (*F*) GCaMP5:mCherry (ΔR/R) ratio traces of vulval muscle Ca^{2+} activity at
836 L4.7-8 (top), L4.9 (middle), and in adults (bottom) during distinct inactive (grey) and active
837 (yellow) egg-laying states. Uncoordinated transients are indicated by blue circles (°),
838 coordinated transients by orange carets (^), egg-laying events by black arrowheads. (*G*
839 and *H*) Cumulative distribution plots of instantaneous vulval muscle Ca^{2+} transient peak
840 frequencies (*G*) and amplitudes (*H*) at L4.7-8 (pink), L4.9 (blue), and in the egg-laying
841 inactive (green) and active state (orange) of adults. Asterisks indicate $p<0.0001$; n.s.
842 indicates $p>0.9999$ (Kruskal-Wallis test). (*I*) Scatterplots show time spent by 9-10 animals
843 with frequent Ca^{2+} transients (inter-transient intervals ≤60 s) at L4.7-8 (pink), L4.9 (blue),
844 and in adults (gray). Error bars show 95% confidence interval for the mean. Asterisks
845 indicates $p\leq0.0002$ (one-way ANOVA). (*J*) Scatterplots show percent synchronous
846 anterior and posterior vulval muscle Ca^{2+} transients in each individual at L4.7-8 (pink),
847 L4.9 (blue), and in adult egg-laying inactive (green) and active states (orange) in wildtype
848 (top) and *egl-1(n986dm)* animals (red) lacking HSNs (bottom). Error bars show 95%
849 confidence intervals for the mean from ≥5 animals. Asterisks indicate $p\leq0.0022$; n.s.
850 indicates $p\geq0.1653$ (one-way ANOVA).

851

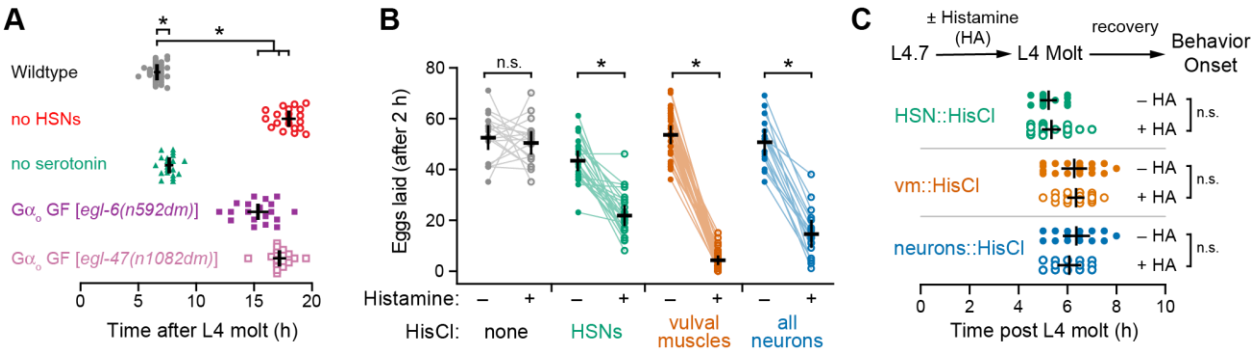

852

853 **Fig. 4. Early HSN and vulval muscle activity is not required for the onset of egg-**
854 **laying behavior**. (*A*) Scatter plots of the first egg-laying event in wild-type (grey), HSN-
855 deficient *egl-1(n986dm)* (red open circles), serotonin-deficient *tph-1(mg280)* (green
856 triangles), *egl-6(n592dm)* (purple squares), and *egl-47(n1082dm)* (pink open squares)
857 mutant animals. Error bars show 95% confidence intervals for the mean from ≥19 animals.
858 Asterisks indicate $p \leq 0.0016$ (One-way ANOVA). (*B*) Scatter plots showing eggs laid by
859 three 24-hour adult animals in two hours before (closed circles) and after incubation with
860 10 mM histamine (open circles). Transgenic animals expressing HisCl in vulval muscles
861 (orange), HSN neurons (green), and all neurons (blue) were compared with the non-
862 transgenic wild-type (grey). Error bars indicate 95% confidence intervals for the mean
863 from ≥17 paired replicates. Asterisks indicate $p<0.0001$; n.s. indicate $p=0.5224$ (paired
864 Student's t test). (*C*) Top, transgenic L4.7 animals were incubated on NGM plates with or
865 without 10 mM histamine until the L4-Adult molt. Animals were then moved to plates
866 lacking histamine and allowed to recover and lay eggs. Bottom, scatter plots show the
867 timing of the first egg-laying event with (open circles) and without (closed circles)
868 histamine. Error bars indicate 95% confidence intervals for the mean; n.s. indicates
869 $p>0.9999$ (one-way ANOVA).

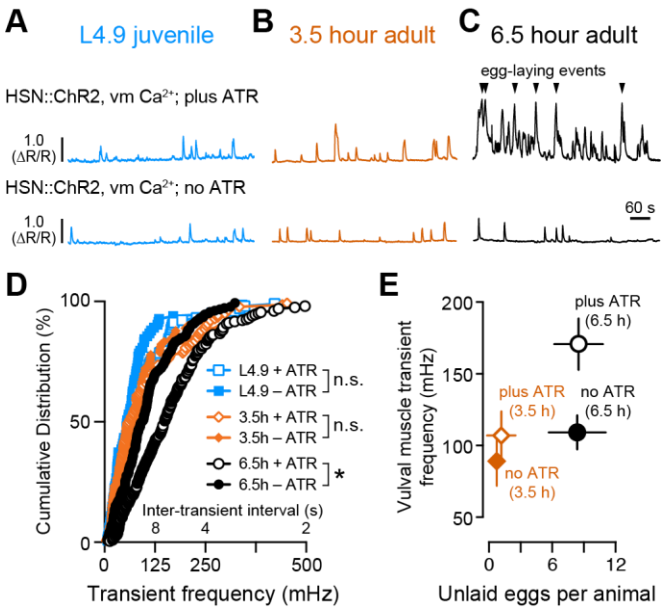

Fig. 5. Unlaid eggs promote vulval muscle responsiveness to HSN activity. (*A-C*) Traces of vulval muscle Ca^{2+} activity at the L4 stage (A, blue), 3.5-hour adults (B, orange), and 6.5-hour adults (C, black) after optogenetic activation of HSN. Animals were grown in the presence (plus ATR, top) or absence (no ATR, bottom) of all-*trans* retinal. 489 nm laser light was used to simultaneously stimulate HSN ChR2 activity and excite GCaMP5 fluorescence for the entire recording. Arrowheads indicate egg laying events. (*D*) Cumulative distribution plots of instantaneous peak frequencies (and inter-transient intervals) of vulval muscle Ca^{2+} activity in L4.9 juveniles (blue filled squares, no ATR; blue open squares, plus ATR), 3.5-hour old adults (orange filled circles, no ATR; orange open circles, plus ATR), and 6.5-hour old adults (black filled circles, no ATR; black open circles, plus ATR). Asterisk indicates $p<0.0001$; n.s. indicates $p\geq0.3836$ (Kruskal-Wallis test). (*E*) Plot shows the average number of unlaid eggs present in the uterus and the average vulval muscle Ca^{2+} transient peak frequency in 3.5-hour old adults (orange closed diamond, no ATR; orange open diamond, plus ATR), and 6.5-hour old adults (black

885 closed diamond, no ATR; black open diamond plus ATR). Error bars indicate 95%
886 confidence intervals for the means.

887

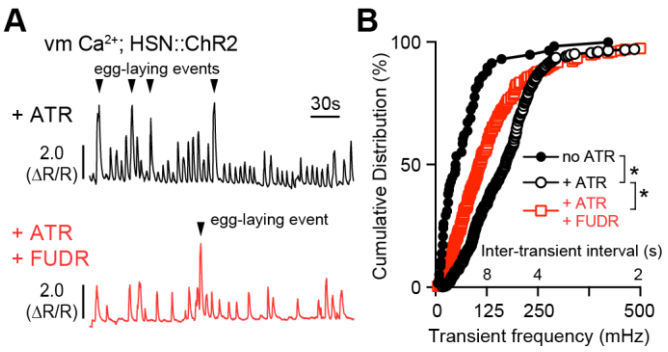

888

889 **Fig. 6. Sterilization decreases vulval muscle responsiveness to HSN activity**. (*A*)
890 Traces of HSN-induced vulval muscle Ca^{2+} activity in untreated (top, black) and FUDR-
891 treated 24-hour adult animals (bottom, red). Arrowheads indicate egg laying events. (*B*)
892 Cumulative distribution plots of instantaneous peak frequencies (and inter-transient
893 intervals) of vulval muscle Ca^{2+} activity after optogenetic activation of HSNs in untreated
894 animals grown with ATR (+ATR, open black circles), FUDR-treated animals with ATR
895 (+ATR, open red circles), and in untreated animals without ATR (no ATR, closed black
896 circles). Asterisks indicate $p<0.0001$ (Kruskal-Wallis test).

897

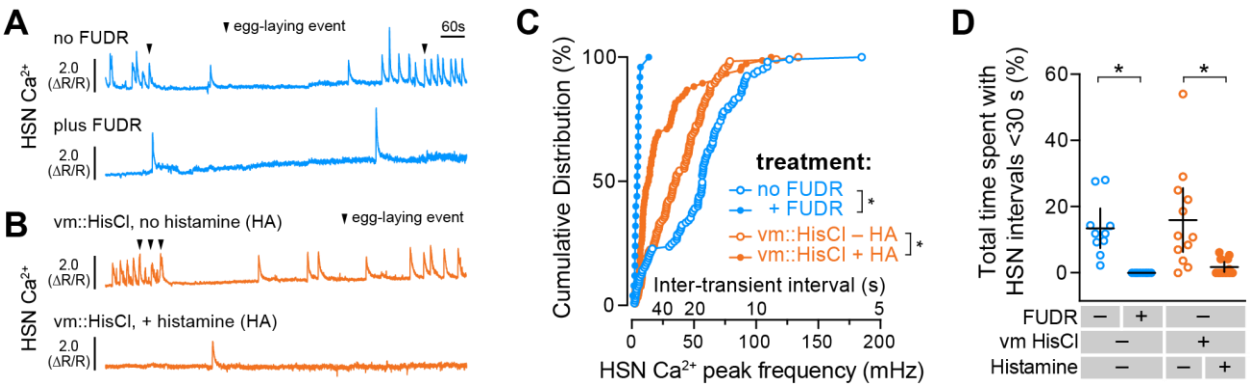

Fig. 7. Egg accumulation and vulval muscle activity promote presynaptic HSN activity. (*A*) HSN Ca^{2+} traces in untreated (top) and FUDR-treated (bottom) adult animals. (*B*) HSN Ca^{2} traces in adult animals expressing HisCl in the vulval muscles (vm) without (top) and after 10 mM histamine treatment (bottom). Arrowheads indicate egg-laying events. (*C*) Cumulative distribution plots of instantaneous HSN Ca^{2+} transient peak frequencies (and inter-transient intervals) of adult HSN Ca^{2+} activity. (*D)* Scatterplots show total time spent by each individual with HSN transients ≤30s apart in FUDR (blue open circles), FUDR-treated (blue closed circles), no histamine (orange open circles), and histamine-silenced vulval muscles (orange closed circles). Asterisks indicate $p \leq 0.0031$ (Kruskal-Wallis test). Error bars indicate 95% confidence intervals for the mean.

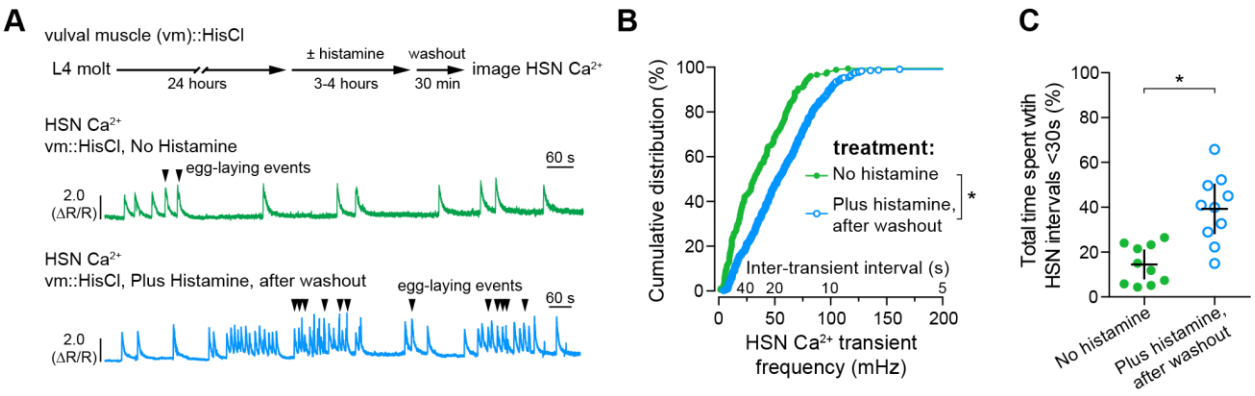

910

911 **Fig. 8. Egg accumulation drives a homeostatic increase in HSN activity and egg**
912 **release.** (*A*) 24-hour old adult animals expressing HisCl in the vulval muscles (vm) and
913 GCaMP5/mCherry in the HSNs were placed onto NGM plates with (blue, bottom) or
914 without histamine (green, top) for 3-4 hours to induce silencing and cessation of egg
915 laying. Animals were then moved to plates without histamine and allowed to recover for
916 30 minutes before HSN Ca^{2+} imaging. Arrowheads indicate egg laying events. (*B*)
917 Cumulative distribution plots of instantaneous HSN Ca^{2+} transient peak frequencies (and
918 inter-transient intervals) after histamine washout (blue open circles) compared with
919 untreated controls (green closed circles). Asterisks indicate $p<0.0001$ (Mann-Whitney
920 test). (*C*) Scatter plots show fraction of time spent by each individual with frequent HSN
921 Ca^{2+} transients characteristic of the egg-laying active state (<30 s) in untreated controls
922 (green circles) and after histamine washout (blue open circles). Error bars indicate 95%
923 confidence intervals for the mean. Asterisk indicates $p=0.0005$ (Student's t test).

924

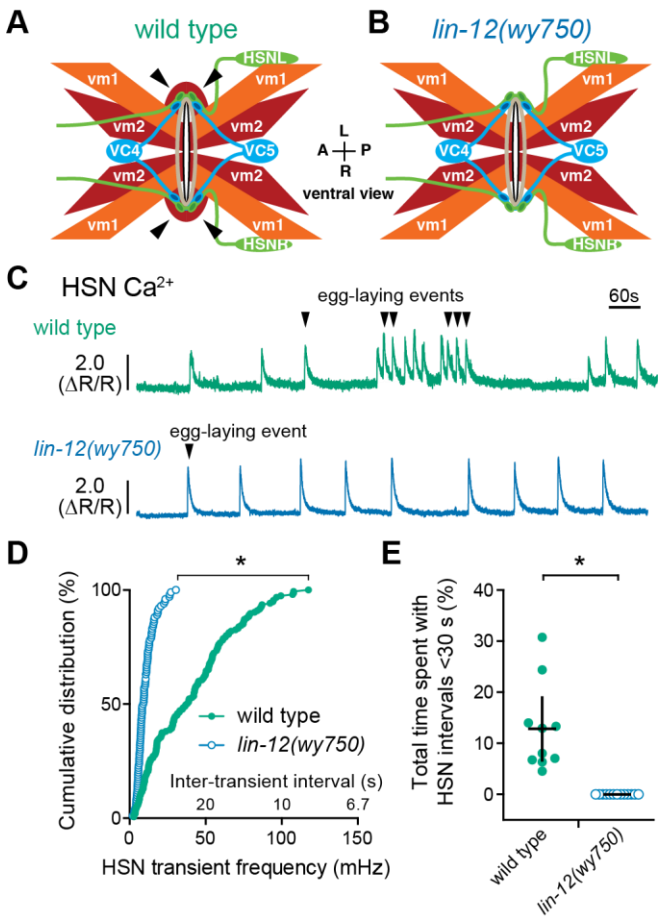

925

926 **Fig. 9: The vm2 muscle arms are required for vulval muscle feedback to HSN and**
927 **burst firing.** (*A-B*) Cartoon of egg-laying circuit structure (lateral view) in wild-type (*A*)
928 and *lin-12(wy750)* mutant (*B*) animals missing lateral vm2 muscle arms (arrowheads). (*C*)
929 Traces show HSN Ca^{2+} activity in wild-type (green) and *lin-12(wy750)* mutant animals
930 (blue). Arrowheads indicate egg-laying events. (*D*) Cumulative distribution plots of
931 instantaneous Ca^{2+} transient peak frequencies (and inter-transient intervals) in wild-type
932 (green circles) and *lin-12(wy750)* mutants (blue circles). Asterisks indicate $p<0.0001$
933 (Mann Whitney test). (*E*) Scatter plots show fraction of time spent by each individual with
934 frequent HSN Ca^{2+} transients characteristic of the egg-laying active state (<30 s) in wild-
935 type (green circles) and *lin-12(wy750)* mutant animals (blue open circles). Error bars

936 indicate 95% confidence intervals for the mean. Asterisk indicates p=0.0011 (Student's t

937 test).

938

SI Materials and Methods

Plasmid and strain construction. A complete list of strains and their use in specific data Figures can be found in Table S1.

Vulval Muscle Ca^{2+}: To visualize vulval muscle Ca^{2+} activity in adult animals, we used LX1918 *vsIs164* [*unc-103e::GCaMP5::unc-54 3'UTR + unc-103e::mCherry::unc-54 3'UTR + lin-15(+)*] *lite-1(ce314) lin-15(n765ts) X* strain as described (1). In this strain, GCaMP5G (2) and mCherry are expressed from the *unc-103e* promoter (3). The *unc-103e* promoter is only weakly expressed in vulval muscles during the L4 stages. To visualize vulval muscle activity in L4 animals, we expressed GCaMP5G and mCherry from the *ceh-24* promoter (4). A ~2.8 kB DNA fragment upstream of the *ceh-24* start site was amplified from genomic DNA by PCR using the following oligonucleotides: 5'-GCG GCA TGC AAC GAG CCA TCC TAT ATC GGT GGT CCT CCG-3' and 5'-CAT CCC GGG TTC CAA GGC AGA GAG CTG CTG-3'. This DNA fragment was ligated into pKMC257 (mCherry) and pKMC274 (GCaMP5G) from which the *unc-103e* promoter sequences were excised to generate pBR3 and pBR4, respectively. pBR3 (20 ng/µl) and pBR4 (80ng/µl) were injected into LX1832 *lite-1(ce314) lin-15(n765ts) X* along with the pLI5EK rescue plasmid (50 ng/µl) (5). The extrachromosomal transgene produced was integrated using UV/TMP creating two independent transgenes *keyIs12* and *keyIs13*, which were then backcrossed to LX1832 parental line six times to generate the strains MIA51 and MIA53. Strain MIA51 *keyIs12* [*ceh-24::GCaMP5::unc-54 3'UTR + ceh-24::mCherry::unc-54 3'UTR + lin-15(+)*] IV; *lite-1(ce314) lin-15 (n765ts) X* was subsequently used for Ca^{2+} imaging. We noted repulsion between *keyIs12* and *wzIs30* IV, a transgene that expresses Channelrhodopsin-2::YFP in HSN from the *egl-6* promoter (6), suggesting both were

linked to chromosome IV. As a result, we crossed MIA53 *keyIs13* [*ceh-24::GCaMP5::unc-54 3'UTR + ceh-24::mCherry::unc-54 3'UTR + lin-15(+)*]*; lite-1(ce314) lin-15(n765ts) X* with LX1836 *wzIs30 IV*; *lite-1(ce314) lin-15(n765ts) X*, generating MIA88 which was used to activate HSN neurons and record vulval muscle Ca^{2+} in L4 animals. In the case of young adults (3 & 6h post molt) and 24h old adults, strain LX1932 *wzIs30 IV; vsIs164 lite-1(ce314) lin-15(n765ts) X* was used as described (1).

HSN Ca^{2+}: To visualize HSN Ca^{2+} activity in L4 and adult animals, we used the LX2004 *vsIs183* [*nlp-3::GCaMP5::nlp-3 3'UTR + nlp-3::mCherry::nlp-3 3'UTR + lin-15(+)*] *lite-1(ce314) lin-15(n765ts) X* strain expressing GCaMP5 and mCherry from the *nlp-3* promoter as previously described (1). In order to visualize HSN Ca^{2+} activity in *lin-12(wy750)* mutant animals lacking post-synaptic vm2 vulval muscle arms, we crossed the MIA194 *lin-12(wy750) III* with LX2004 *vsIs183 lite-1(ce314) lin-15(n765ts) X* to generate MIA196 *lin-12(wy750) III*; *vsIs183 X lite-1(ce314) lin-15 (n765ts) X.*

Vulval muscle HisCl: To produce a vulval muscle-specific HisCl transgene, coding sequences for mCherry in pBR3 were replaced with that for HisCl. First, an EagI restriction site (3' of the mCherry encoding sequence) was changed to a NotI site using Quickchange mutagenesis to generate pBR5. The ~1.2 kB DNA fragment encoding the HisCl channel was amplified from pNP403 (7) using the following oligonucleotides: 5'-GCG GCT AGC GTA GAA AAA ATG CAA AGC CCA ACT AGC AAA TTG G-3' and 5'-GTG GCG GCC GCT TAT CAT AGG AAC GTT GTC-3', cut with NheI/NotI, and ligated into pBR5 to generate pBR7. pBR7 (80ng/µl) was injected into LX1832 along with pLI5EK (50ng/µl). One line bearing an extrachromosomal transgene was integrated with UV/TMP, and six independent integrants (*keyIs14* to *keyIs19*) were recovered. Four of these were

985 then backcrossed to the LX1832 parental line six times to generate strains MIA68, MIA69,
986 MIA70, and MIA71. All four strains were used for behavioral assays in adult animals to
987 test the effect of vulval muscle silencing on egg laying (Fig. 4B). MIA71 *keyIs19* [*ceh-*
988 *24::HisCl::unc-54 3'UTR + lin-15(+)*]*; lite-1(ce314) lin-15(n765ts) X* strain was used to
989 study the effect of acute silencing of early activity on egg-laying behavior (Fig. 4C). To
990 visualize HSN Ca^{2+} activity after vulval muscle silencing, we crossed MIA71 with LX2004
991 to generate strain MIA80 *keyIs19; vsIs183 lite-1(ce314) lin-15(n765ts) X.*
992 ***HSN HisCl:*** The ~1.2 kB DNA fragment encoding the HisCl channel was amplified from
993 pNP403 using the following oligonucleotides: 5'- GCG GCT AGC GTA GAA AAA ATG
994 CAA AGC CCA ACT AGC AAA TTG G-3' and 5'-GCG GAG CTC TTA TCA TAG GAA
995 CGT TGT CCA ATA GAC AAT A-3'. The amplicon was digested with NheI/SacI and
996 ligated into similarly cut pSF169 (*pegl-6*::mCre (8)) to generate pBR10. To follow
997 expression in HSN, mCherry was amplified using the following oligonucleotides: 5'- GCG
998 GCT AGC GTA GAA AAA ATG GTC TCA AAG GGT-3' and 5'- GCG GAG CTC TCA
999 GAT TTA CTT ATA CAA TTC ATC CAT G-3'. This amplicon was digested with NheI/SacI
1000 and ligated into pSF169 to generate pBR12. pBR10 (HisCl; 5ng/µl) and pBR12 (mCherry;
1001 10ng/µl) were injected into LX1832 *lite-1(ce314) lin-15(n765ts)* along with pLI5EK
1002 (50ng/µl). The extrachromosomal transgene produced was integrated with UV/TMP,
1003 creating three independent integrants (*keyIs20* to *keyIs22*). The resulting animals were
1004 backcrossed to the LX1832 parental line six times to generate strains MIA115, MIA116,
1005 and MIA117. The MIA116 strain had a low incidence of HSN developmental defects and
1006 was used subsequently for behavioral assays.

All neuron HisCl: pNP403 was injected into LX1832 *lite-1(ce314) lin-15(n765ts)* animals at 50ng/µl along with pLI5EK (50ng/µl) to produce strain MIA60 carrying extrachromosomal transgene *keyEx16* [*tag-168::HisCl::SL2::GFP* + *lin15(+)*]. Non-Muv, *lin-15(+)* animals with strong GFP expression in the HSNs and other neurons were selected prior to behavioral silencing assays. All selected animals showed histamine-dependent paralysis that recovered after washout.

Vulval muscle morphology: To visualize vulval muscle development at the L4 stages, we injected pBR3 (80ng/µl) [*pceh-24*::mCherry] along with a co-injection marker pCFJ90 (10ng/µl) into TV201 *wyIs22* [*punc-86*::GFP::RAB-3 + *podr-2*::dsRed] (9) to generate an extrachromosomal transgene, *keyEx42*. To visualize adult vulval muscle morphology, we used the LX1918 *vsIs164* [*unc-103e::GCaMP5::unc-54 3'UTR* + *unc-103e::mCherry::unc-54 3'UTR* + *lin-15(+)*] *lite-1(ce314) lin-15(n765ts) X* strain (1). To visualize the expression of the *ser-4* gene, we used the strain AQ570 [*ijIs570*] (10, 11).

HSN morphology: We used the LX2004 strain expressing mCherry from the *nlp-3* promoter to visualize HSN morphology at L4 stages as well as in adults. To visualize HSN presynaptic development at L4 stages, the *wyIs22* transgene was used.

Whole circuit morphology (HSN, VC and uv1 cells): A ~3.2 kB DNA fragment upstream of the *ida-1* start site (12) was cloned using the following oligonucleotides: 5'-GCG GCA TGC CCT GCC TGT GCC AAC TTA CCT-3' and 5'-CAT CCC GGG GCG GAT GAC ACA GAG ATG CGG-3'. The DNA fragment was digested with SphI/XmaI and ligated into pKMC257 and pKMC274 to generate plasmids pBR1 and pBR2. pBR1 (20 ng/µl) and pBR2 (80ng/µl) were co-injected into LX1832 along with pLI5EK (50 ng/µl). The extrachromosomal transgene produced was integrated with UV/TMP creating four

independent integrants *keyIs8* to *keyIs11,* which were then backcrossed to LX1832 parental line six times. MIA49 *keyIs11* [*ida-1::GCaMP5::unc-54 3'UTR* + *ida-1::mCherry::unc-54 3'UTR* + *lin-15(+)*]; *lite-1(ce314) lin-15 (n765ts) X* was used subsequently to visualize whole-circuit morphology.

Optogenetics and Defecation Behavior Assays.

Intervals between Expulsion steps of the defecation motor program were determined as described from brightfield and HSN Ca^{2+} recordings (13). To test whether optogenetic activation of the HSNs affected defecation behavior on plates, a OTPG_4 TTL Pulse Generator (Doric Optics) was used to trigger image capture (Grasshopper 3, 4.1 Megapixel, USB3 CMOS camera, Point Grey Research) and shutter opening on a EL6000 metal halide light source generating 8-16 mW/cm^2 of ~470±20nm blue light via a EGFP filter set mounted on a Leica M165FC stereomicroscope. Late L4 and adult LX1836 transgenic animals were maintained on OP50 seeded with or without all-*trans* retinal (ATR) (0.4 mM). Animals were illuminated with blue light for a duration of 2 minutes, and video recordings of defecation events which occurred within the duration of blue light activation were obtained.

Supplemental references

1. Collins KM, *et al.* (2016) Activity of the *C. elegans* egg-laying behavior circuit is controlled by competing activation and feedback inhibition. *Elife* 5:e21126.
2. Akerboom J, *et al.* (2013) Genetically encoded calcium indicators for multi-color neural activity imaging and combination with optogenetics. *Front Mol Neurosci* 6:2.
3. Collins KM & Koelle MR (2013) Postsynaptic ERG potassium channels limit muscle excitability to allow distinct egg-laying behavior states in *Caenorhabditis elegans*. *J Neurosci* 33(2):761-775.
4. Harfe BD & Fire A (1998) Muscle and nerve-specific regulation of a novel NK-2 class homeodomain factor in *Caenorhabditis elegans*. *Development* 125(3):421-429.
5. Clark SG, Lu X, & Horvitz HR (1994) The *Caenorhabditis elegans* locus lin-15, a negative regulator of a tyrosine kinase signaling pathway, encodes two different proteins. *Genetics* 137(4):987-997.
6. Emtage L, *et al.* (2012) IRK-1 potassium channels mediate peptidergic inhibition of *Caenorhabditis elegans* serotonin neurons via a G(o) signaling pathway. *J Neurosci* 32(46):16285-16295.
7. Pokala N, Liu Q, Gordus A, & Bargmann CI (2014) Inducible and titratable silencing of *Caenorhabditis elegans* neurons in vivo with histamine-gated chloride channels. *Proc Natl Acad Sci U S A* 111(7):2770-2775.
8. Flavell SW, *et al.* (2013) Serotonin and the neuropeptide PDF initiate and extend opposing behavioral states in *C. elegans*. *Cell* 154(5):1023-1035.
9. Patel MR, *et al.* (2006) Hierarchical assembly of presynaptic components in defined *C. elegans* synapses. *Nat Neurosci* 9(12):1488-1498.
10. Gurel G, Gustafson MA, Pepper JS, Horvitz HR, & Koelle MR (2012) Receptors and other signaling proteins required for serotonin control of locomotion in *Caenorhabditis elegans*. *Genetics* 192(4):1359-1371.
11. Tsalik EL & Hobert O (2003) Functional mapping of neurons that control locomotory behavior in *Caenorhabditis elegans*. *J Neurobiol* 56(2):178-197.
12. Cai T, Fukushige T, Notkins AL, & Krause M (2004) Insulinoma-Associated Protein IA-2, a Vesicle Transmembrane Protein, Genetically Interacts with UNC-31/CAPS and Affects Neurosecretion in *Caenorhabditis elegans*. *J Neurosci* 24(12):3115-3124.
13. Thomas JH (1990) Genetic analysis of defecation in Caenorhabditis elegans. *Genetics* 124(4):855-872.

Supplementary Figures and Tables

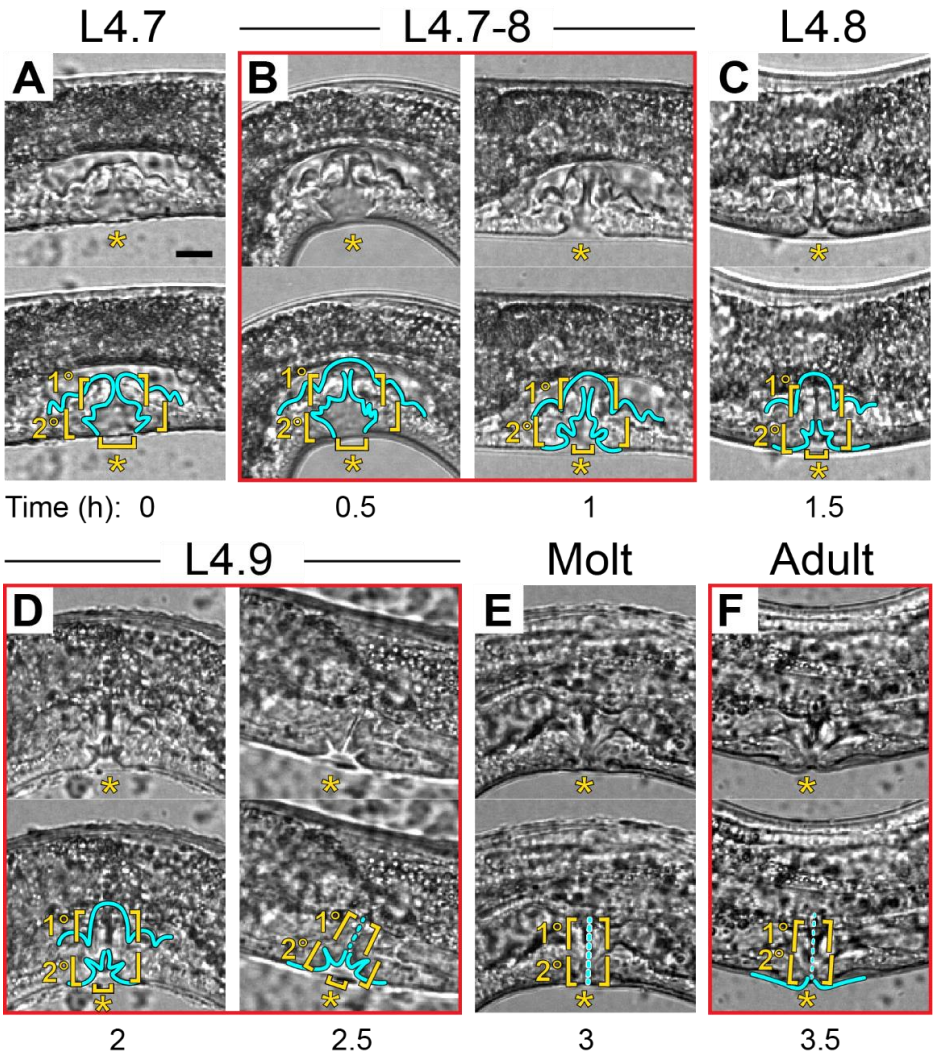

Fig. S1: Morphological development of the *C. elegans* egg-laying circuit. (*A-F*) Representative images of vulval morphology at late L4 stages- (*A*) L4.7, (*B*) L4.7-8, (*C*) L4.8, (*D*) L4.9, (*E*) Molt and (*F*) Young adult. Cartoon trace (cyan) in panels shows the gross morphology of the developing vulva at each stage. Yellow horizontal square brackets (yellow) near the vulval opening indicate the width of the vulval lumen. Yellow vertical square brackets encompass the length of primary (1°) vulval epithelial (vulE and vulF) and secondary (2°) vulval epithelial (vulA-D) cells. Anterior is at left and ventral is at

bottom. Scale bar in all images is 10 µm, and asterisk indicates the position of the developing or completed vulval opening.

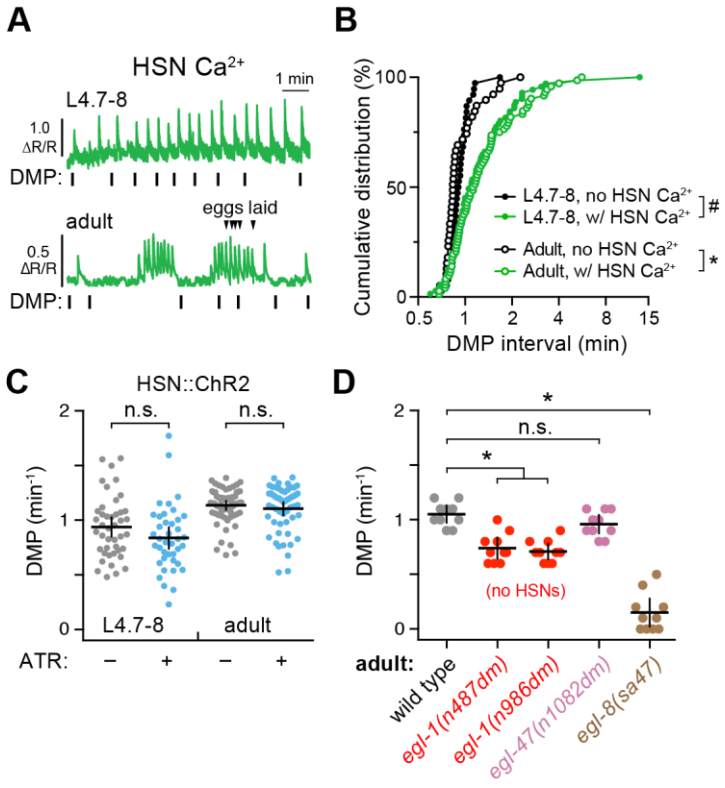

Fig. S2: HSN regulates the defecation motor program. (*A*) Representative HSN Ca^{2+} traces at the L4.7-8 larval stage (top) and adults (bottom). Vertical lines indicate the expulsion step of the defecation motor program (DMP); arrowheads indicate adult egg-laying events. (B) Cumulative distribution plots showing DMP intervals with no HSN Ca^{2+} transient (black) versus those with one or more HSN Ca^{2+} transients (green) in L4.7-8 (closed circles) and adult (open circles). Pound indicates p=0.0058; asterisk indicates p<0.0001 (Kruskal-Wallis test with Dunn's correction for multiple comparisons). (*C*) Scatter plots showing the consequences of HSN optogenetic activation on the DMP frequency. L4.7-8 and adult animals expressing Channelrhodpsin-2 in HSN neurons were grown in the absence (-, grey) or presence (+, blue) of all-*trans* retinal (ATR), illuminated with blue light for two minutes, and the timing of DMP events was used to calculate an instantaneous DMP frequency. Error bars show 95% confidence intervals for the mean;

1112 n.s. indicates p=0.0645 (L4.7-8) or p=0.1866, (adult) (Student's t test). (*D*) Scatter plots
1113 showing DMP frequencies (min^{-1}) in wild-type (grey), *egl-1(n487dm)* and *egl-1(n986dm)*
1114 (red), *egl-47(n1082dm)* (pink), and *egl-8(sa47)* (brown) adults. Error bars indicate the
1115 95% confidence interval for the mean. Asterisk indicates p<0.0001; n.s. indicates
1116 p=0.5208 (One-way ANOVA with Bonferroni's correction for multiple comparisons).
1117

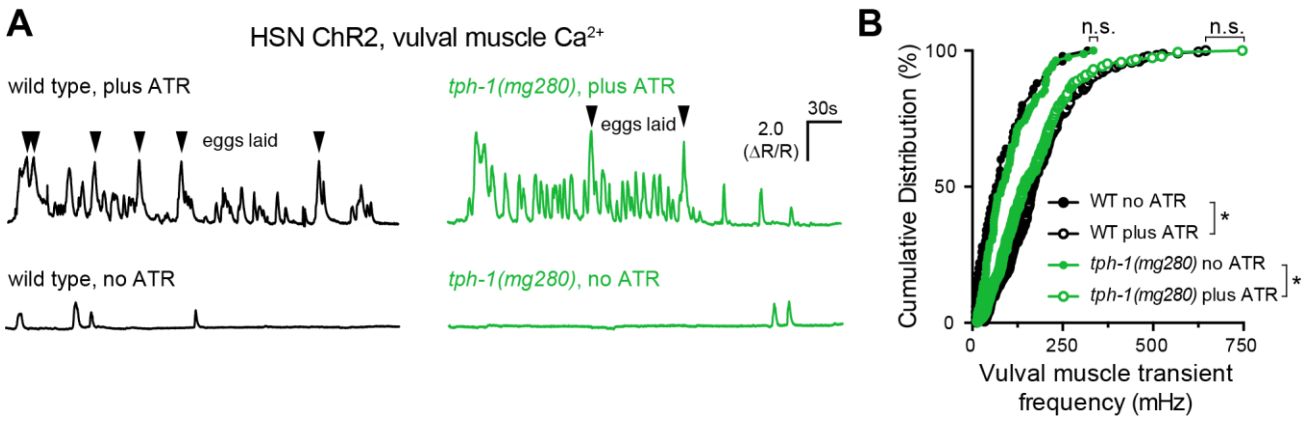

Fig. S3. HSN activation of the vulval muscles does not require serotonin. (A) Vulval muscle Ca^{2+} recordings from 6-hour adult wild-type and *tph-1(mg280)* mutant animals expressing Channelrhodopsin-2 (ChR2) in the HSNs grown in the presence (plus ATR, top) or absence (no ATR, bottom) of all-*trans* retinal. 489 nm laser light was used to simultaneously stimulate ChR2 activity and excite GCaMP5 fluorescence during the entire recording. Arrowheads indicate egg-laying events. (*B*) Cumulative distribution plots of instantaneous vulval muscle Ca^{2+} transient peak frequencies of 6-hour adult wild-type (black filled circles, no ATR; black open circles, plus ATR) and *tph-1(mg280)* mutant animals (green filled circles, no ATR; green open circles, plus ATR). Asterisks indicate $p<0.0001$; n.s. indicates $p\geq0.2863$ (Kruskal-Wallis test with Dunn's correction for multiple comparisons).

Strain	Feature	Genotype	Figures
LX1832	Strain for transgene production	*lite-1(ce314) lin-15(n765ts) X*	-
N2	Bristol strain	wild type	4, S1, S2
LX2004	HSN GCaMP5, mCherry	*vsIs183 lite-1(ce314) lin-15(n765ts) X*	1, 2, 7, 9, S2
TV201	HSN presynaptic RAB-3-GFP	*wyIs22 IV*	1
MIA189	mCherry expression under *ceh-24* promoter	*keyEx40; wyIs22 IV*	1
LX1918	vulval muscles GCaMP5, mCherry	*vsIs164 lite-1(ce314) lin-15(n765ts) X*	1, 3
AQ570	GFP expression under the *ser-4* promoter	*ijIs570*	1
MIA49	HSN, VC and uv1 cells GCaMP5, mCherry	*keyIs11; lite-1(ce314) lin-15(n765ts) X*	1
MIA51	Vulval muscles GCaMP, mCherry (under *ceh-24* promoter)	*keyIs12; lite-1(ce314) lin-15(n765ts) X*	3
LX1938	No HSNs, vulval muscles GCaMP5, mCherry	*egl-1(n986dm) V*; *vsIs164 lite-1(ce314) lin-15(n765ts) X*	3
MIA78	No HSNs, vulval muscles GCaMP5, mCherry	*egl-1(n986dm) V*; *keyIs12; lite-1(ce314) lin-15(n765ts) X*	3
MT2059	No HSNs	*egl-1(n986dm) V*	4, S2
MT1222	Increased $G\alpha_o$ signaling in HSN	*egl-6(n5920) X*	4
MT2258	Increased $G\alpha_o$ signaling in HSN	*egl-47(n1081) V*	4, S2
MT15434	No serotonin	*tph-1(mg280) II*	4
MIA71	vulval muscles expressing Histamine-gated Cl^- channels (HisCl)	*keyIs19; lite-1(ce314) lin-15(n765ts) X*	4
MIA116	HSN HisCl	*keyIs21; lite-1(ce314) lin-15(n765ts) X*	4
MIA60	All neurons HisCl	*keyEx16; lite-1(ce314) lin-15(n765ts) X*	4
MIA88	HSN Channelrhodopsin, vulval muscle GCaMP5, mCherry (under *ceh-24* promoter)	*wzIs30 IV*; *keyIs13; lite-1(ce314) lin-15(n765ts) X*	5
LX1932	HSN Channelrhodopsin, vulval muscle GCaMP5, mCherry (under *unc-103e* promoter)	*wzIs30 IV*; *vsIs164 lite-1(ce314) lin-15(n765ts) X*	5, 6, S3
MIA80	Vulval muscles HisCl, HSN GCaMP5, mCherry	*keyIs19; vsIs183 lite-1(ce314) lin-15(n765ts) X*	7, 8
MIA196	No vulval muscle arms, HSN GCaMP, mCherry	*lin-12(wy750) III; vsIs183 lite-1(ce314) lin-15(n765ts) X*	9
MT1082	No HSNs	*egl-1(n487) V*	S2
JT47	PLCβ null mutant, infrequent defecation	*egl-8(sa47) V*	S2
LX1836	HSN Channelrhodopsin	*wzIs30 IV*; *lite-1(ce314) lin-15(n765ts) X*	S2
MIA191	*tph-1* null mutant HSN Channelrhodopsin, vulval muscle GCaMP5, mCherry (under *unc-103e* promoter)	*tph-1(mg280) II; wzIs30 IV*; *vsIs164 lite-1(ce314) lin-15(n765ts) X*	S3

Table S1. All strains are derived from the Bristol N2 genetic background and are listed above.

Supplemental Movie legends

Movie S1. Ratio recording of a HSN Ca^{2+} transient at the L4.9 larval stage. High Ca^{2+} is indicated in red while low calcium is in blue. The HSN cell body and pre-synaptic terminal are indicated. Head is at bottom, tail is at left.

Movie S2. Ratio recording of a HSN Ca^{2+} transient prior to an egg-laying event in an adult animal during the active state. High Ca^{2+} is indicated in red while low calcium is in blue. The HSN cell body and pre-synaptic terminal are indicated. Head is at bottom, tail is at top.

Movie S3. Ratio recording of an uncoordinated vulval muscle Ca^{2+} transient at the L4.7-8 larval stage. High Ca^{2+} is indicated in red while low calcium is in blue. Developing anterior and posterior vulval muscles are indicated. Head is at top, tail is at bottom.

Movie S4. Ratio recording of an uncoordinated vulval muscle Ca^{2+} transient at the L4.9 larval stage. High Ca^{2+} is indicated in red while low calcium is in blue. Anterior and posterior vulval muscles are indicated. Head is at left, tail is at bottom.

Movie S5. Ratio recording of a coordinated vulval muscle Ca^{2+} transient at the L4.9 larval stage. High Ca^{2+} is indicated in red while low calcium is in blue. Anterior and posterior vulval muscles are indicated. Head is at top, tail is at bottom.

Movie S6. Ratio recording of coordinated vulval muscle Ca^{2+} transients during egg laying in adult animals. High Ca^{2+} is indicated in red while low calcium is in blue. The anterior and posterior vulval muscles are indicated along with a previously laid egg. Head is at right, tail is at left.